CellPress

Neuron
Article

A Role for *Tac2*, NkB, and Nk3 Receptor in Normal and Dysregulated Fear Memory Consolidation

Raül Andero,[1,2,*] Brian G. Dias,[1,2] and Kerry J. Ressler[1,2,3]
[1]Department of Psychiatry and Behavioral Sciences, Emory University School of Medicine, Atlanta, GA 30329, USA
[2]Center for Behavioral Neuroscience, Yerkes National Primate Research Center, Atlanta, GA 30329, USA
[3]Howard Hughes Medical Institute, Bethesda, MD 20814, USA
*Correspondence: raul.andero.gali@gmail.com
http://dx.doi.org/10.1016/j.neuron.2014.05.028

SUMMARY

The centromedial amygdala (CeM), a subdivision of the central amygdala (CeA), is believed to be the main output station of the amygdala for fear expression. We provide evidence that the *Tac2* gene, expressed by neurons specifically within the CeM, is required for modulating fear memories. *Tac2* is colocalized with GAD65 and CaMKIIα but not with *PKCd* and *Enk* neurons in the CeM. Moreover, the *Tac2* product, NkB, and its specific receptor, Nk3R, are also involved in the consolidation of fear memories. Increased *Tac2* expression, through a stress-induced PTSD-like model, or following lentiviral CeA overexpression, are sufficient to enhance fear consolidation. This effect is blocked by the Nk3R antagonist osanetant. Concordantly, silencing of *Tac2*-expressing neurons in CeA with DREADDs impairs fear consolidation. Together, these studies further our understanding of the role of the *Tac2* gene and CeM in fear processing and may provide approaches to intervention for fear-related disorders.

INTRODUCTION

Among learning and memory processes, fear memories are crucial in anxiety disorders such as panic disorder, phobia, and posttraumatic stress disorder (PTSD). PTSD occurs in some individuals after experiencing or witnessing extreme traumatic events. The symptoms of PTSD include re-experiencing memories of these traumatic events through intrusive thoughts, flashbacks, and nightmares (American Psychiatric Association, 2013). PTSD is also generally accompanied by hyperarousal symptoms. Moreover, persistent highly aversive memories related to the trauma, potentially overconsolidated memories, and the inability of these memories to be extinguished are all frequent characteristics of this disorder. Specifically relevant is the memory consolidation phase following emotional learning, since it is required to stabilize the initial fear memory trace.

In order to decrease the prevalence of PTSD, it is necessary to identify biological and environmental risk and resilience markers (Norrholm and Ressler, 2009; Vermetten and Lanius, 2012), to find early interventions after trauma exposure (Kearns et al., 2012), and to treat the disorder when it is present and debilitating (Andero and Ressler, 2012; Hetrick et al., 2010). Notably, understanding molecular pathways mediating the initial fear consolidation event is particularly important to target the prevention of PTSD. The only FDA-approved pharmaceutical treatments for PTSD are selective serotonin reuptake inhibitor (SSRI) antidepressants, which have met with limited results in clinical trials (Hetrick et al., 2010). Even when antidepressants are combined with exposure-based psychotherapy, increased effectiveness has not always been demonstrated (Hetrick et al., 2010). Thus, more effective, targeted approaches to prevention and treatment are needed to normalize the functioning of areas key to fear processes such as the amygdala, the hippocampus, or the medial prefrontal cortex (mPFC).

The tachykinins refer to two peptides encoded in rodents by the *Tachykinin* 1 (*Tac1*) and *Tac2* (*TAC3* in humans) genes, which are involved in neurotransmission and neuromodulation in the CNS (Beaujouan et al., 2004). *Tac1* encodes a precursor protein that produces two peptides, substance P (SP) and neurokinin A (NkA), whereas *Tac2*/*TAC3* encodes neurokinin B (NkB). SP and NkA have been previously implicated in fear processes and PTSD (Dunlop et al., 2012). Unfortunately, clinical trials with pharmaceutical agents targeting the *Tac1* pathway have not previously shown beneficial effects in PTSD treatment (Dunlop et al., 2012). A possible explanation for this lack of effect is that the SP and NkA receptors (Neurokinin 1 receptor [Nk1R] and Neurokinin 2 receptor [Nk2R]) are widely expressed in the brain. So, when administering drugs that specifically target Nk1 and Nk2, they interact with multiple brain regions affecting multiple functions (Beaujouan et al., 2004). In contrast, the expression of *Tac2*, NkB, and its specific receptor, Neurokinin 3 receptor (Nk3R), are relatively restricted in rodents to brain regions that regulate emotion, such as the amygdala (Beaujouan et al., 2004; Duarte et al., 2006). Nk3R is a G protein-coupled tachykinin receptor that binds NkB with highest affinity (Gether, 2000; Khawaja and Rogers, 1996). Nk3R couples to the pertussis toxin-insensitive G proteins Gq/G_{11}, the activation of which results in the production of inositol triphosphate and diacylglycerol and the activation of protein kinase C (Khawaja and Rogers, 1996). Additionally, it has been shown that *TAC3* and Nk3R are expressed in the equivalent areas in rhesus monkeys and humans (Mileusnic et al., 1999; Nagano et al., 2006).

Here, beginning with an unbiased discovery approach, we show that the *Tac2* gene is dynamically regulated during the

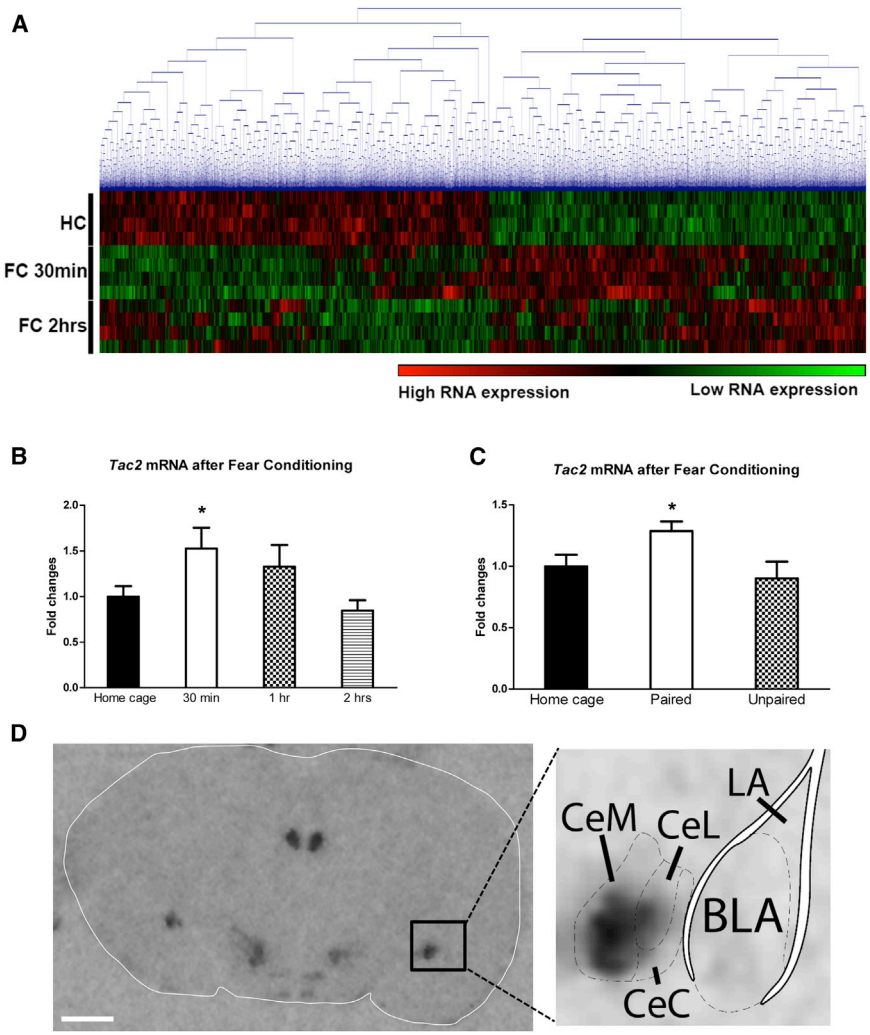

Figure 1. Differential Regulation of *Tac2* Gene Expression in the Amygdala during Cued-Fear Conditioning

(A) With average linkage hierarchical clustering of an RNA microarray, there is a differential gene regulation 30 min and 2 hr after auditory fear conditioning (FC) when compared to home cage group (no FC). n = 4 per group.

(B) *Tac2* mRNA levels are rapidly upregulated in the amygdala during fear consolidation 30 min after fear conditioning. *p $\leq$ 0.05 versus HC and 2 hr. n = 7–8 per group.

(C) *Tac2* upregulation occurs when the conditioned stimulus (acoustic tone) and the unconditioned stimulus (electric footshock) are paired but not when they are unpaired. *p $\leq$ 0.05 versus HC and unpaired. n = 11–15 per group. Mean + SEM is shown.

(D) *Tac2* expression by radioactive in situ hybridization in the amygdala is restricted to the central amygdala (CeA) with highest expression in the CeM amygdala. Scale bar, 1 mm. See also Figure S1 and Tables S1 and S2.

consolidation of conditioned fear within the central amygdala (CeA). Additionally, Nk3R activation is required for normal consolidation of fear memory formation in mice. Furthermore, increased expression of the *Tac2* gene, NkB peptide, and activation of Nk3R may be involved in stress sensitization and overconsolidation of fear. In contrast, genetic silencing of *Tac2*-expressing neurons impairs fear consolidation. Blockade of this pathway may provide for a novel therapeutic approach for disorders with altered fear learning such as PTSD.

RESULTS

Tac2 Is Involved in Fear Learning

Using amygdala tissue punches from mice that had been sacrificed 30 min or 2 hr after auditory fear conditioning (FC) (CS, acoustic tone; US, electric footshocks; Figure S1A available online), we performed an mRNA microarray. Using average linkage hierarchical clustering, the microarray heat map shows differential gene regulation at 30 min and at 2 hr after fear learning, which is a critical period for consolidation of fear memories (Ressler et al., 2002; Figure 1A). False discovery rate (FDR) was calculated with SAM 4.01 using a standard 5% cutoff criteria. The cutoff criteria was set with an FDR at the 1.3-fold level for the 2 hr after fear conditioning (FC) group, since with the more conservative 1.5-fold cutoff used in the 30 min after FC group, no genes were initially identified. The criteria followed in Tables S1 and S2 for a Yes in the column "Specifically highly expressed in the amygdala" is the following: (1) very high expression in the amygdala (red color, Allen Brain Atlas), and (2) no expression of the gene in the hippocampus or PFC (other key areas related to emotional learning). Moreover, from the top candidates of this microarray, the only gene that is specifically highly expressed in the amygdala and belongs to a "druggable" pathway with available agonists and antagonists that cross the blood-brain barrier and can be used systemically is *Tac2* (see Tables S1 and S2; Figures S1B and S2). Therefore, we focused on understanding and manipulating the *Tac2* pathway.

Independent replication studies with additional fear-conditioned mice show that *Tac2* is rapidly upregulated at 30 min after FC, returning to basal levels at 2 hr (ANOVA $F_{3,28} = 5.014$, $p \leq 0.01$, post hoc *p $\leq$ 0.05 versus home cage [HC] and 2 hr; Figure 1B). Moreover, in an additional replication, *Tac2* mRNA upregulation only occurred when the conditioned and unconditioned stimuli are paired but not when they are unpaired, suggesting that within this paradigm, *Tac2*-increased expression is specific to associative cued fear learning and independent of nonspecific stress and/or contextual learning (ANOVA $F_{2,36} = 3.93$, $p \leq 0.05$, post hoc *p $\leq$ 0.05 versus HC and unpaired; Figure 1C). See Figure S3 for detailed interactions of the *Tac2* gene and Nk3R.

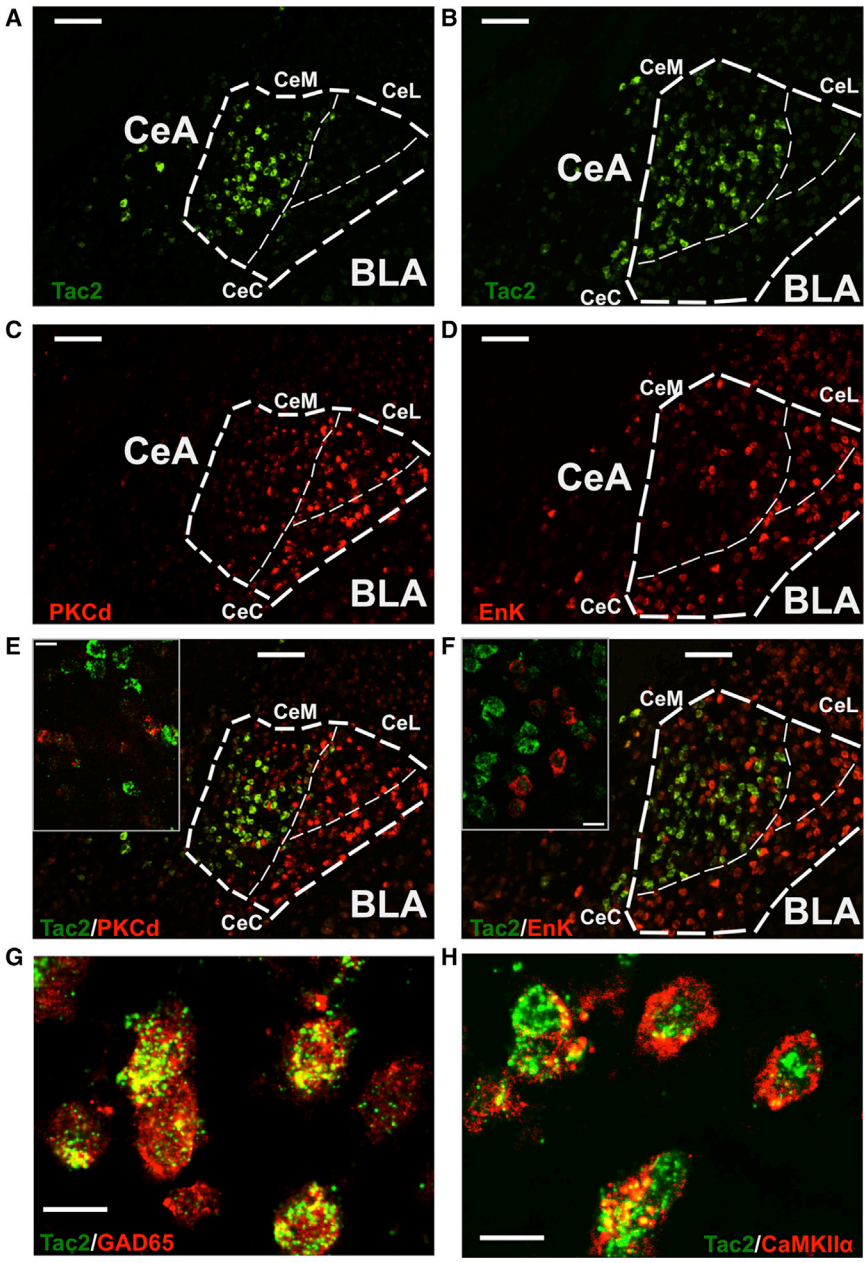

Figure 2. *Tac2* Is Colocalized with Glutamate Decarboxylase 65 and Calmodulin-Dependent Protein Kinase II α but Is Not Colocalized with Protein Kinase C Delta or Enkephalin-Expressing Neurons in the CeM

(A) *Tac2* mRNA expression in the CeA and BLA by nonradioactive fluorescent in situ hybridization (FISH). Scale bar, 100 μm.

(B) *Tac2* mRNA expression by FISH in another coronal section. Scale bar, 100 μm.

(C) *PKCd* mRNA expression by FISH. Scale bar, 100 μm.

(D) *Enk* mRNA expression by FISH. Scale bar, 100 μm.

(E) Right: (A) and (C) merged showing different pattern of expression of *Tac2* and *PKCd* in the CeA. Scale bar, 100 μm. Left: confocal image showing no colocalization of *Tac2* and *PKCd* in the CeM. Scale bar, 15 μm.

(F) Right: (B) and (D) merged showing different pattern of expression of *Tac2* and *Enk*. Scale bar, 100 μm. Left: confocal image showing no colocalization of *Tac2* and *Enk* in the CeM. Scale bar, 15 μm.

(G) Confocal image showing colocalization of *Tac2* mRNA expression and GAD65 peptide in the CeM. Scale bar, 15 μm.

(H) Confocal image showing colocalization of *Tac2* mRNA expression and CaMKIIα peptide in the CeM. Scale bar, 15 μm. CeM, centromedial amygdala; CeL, centrolateral amygdala; CeC, centrocentral amygdala; CeA, central amygdala; BLA, basolateral amygdala.

Tac2, NkB, and Nk3R in the Amygdala

Figures 1D and S1B show a radioactive in situ hybridization demonstrating that the areas where *Tac2* gene is expressed are quite specific and limited within in the mouse brain: bed nucleus of the stria terminalis, hypothalamus, habenula, central amygdala (CeA), zona incerta, and medial mammillary nucleus. *Tac2* is highly expressed in the CeA within the amygdala, with no expression in the basolateral amygdala (BLA) or lateral amygdala (LA) (Figure 1D). The highest expression of *Tac2* within the CeA occurs in the medial subdivision of the central amygdaloid nucleus (CeM), whereas lower expression is observed in the centrolateral (CeL) and centrocentral (CeC) amygdala.

Recently, specific cell populations within the central nucleus have received attention for distinct roles in fear learning. For example, *PKCd* has been suggested to be part of a microcircuit in which the CeL amygdala neurons inhibit neuronal output to the CeM during the conditioned stimulus, which drives fear expression, called CeL_{off} units (Haubensak et al., 2010). Moreover, around 40% of protein kinase C delta (*PKCd*)-expressing neurons also express Enkephalin (*Enk*) in the CeL (Haubensak et al., 2010). Of note, *Enk* mRNA levels are increased after FC in the CeL (Petrovich et al., 2000). Since other neuronal populations have been previously related to fear processes in the CeA, we wished to examine whether *Tac2* mRNA colocalized with them, suggesting functional interactions. Using double fluorescent in situ hybridization (FISH), we show that *Tac2* gene expression is mostly not colocalized with *PKCd* or *Enk* and is expressed primarily within the CeM (Figures 2A–2F). Thus, given the lack of colocalization and regional and functional specificity of these cell populations, we have uncovered a subdivision-specific cell population that may be involved in the consolidation of fear memory. Additionally, the colocalization of *Tac2* mRNA levels and the 65 kDa isoform of glutamic acid decarboxylase (GAD65) peptide in the CeM

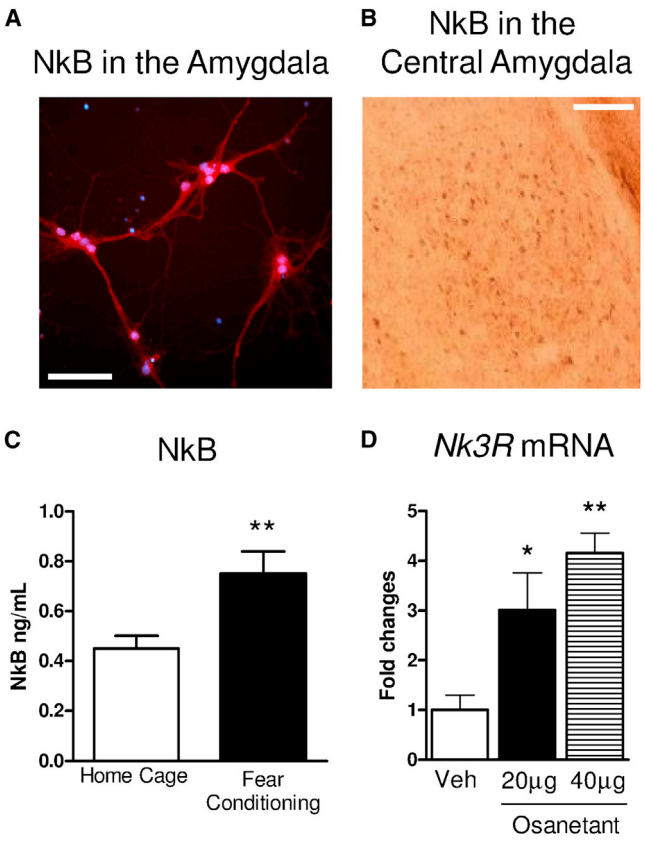

Figure 3. Fear Conditioning, Expression of Neurokinin B and Neurokinin 3 Receptor in the Amygdala

(A) The *Tac2* product Neurokinin B (NkB) is detected by immunocytochemistry in mouse amygdala cell culture. NkB is highly expressed in the soma and in the dendrites. Red represents NkB signal. Blue represents neuronal nucleus, NeuN. Scale bar, 25 μm.

(B) Immunohistochemistry studies show high expression of NkB in the central amygdala (CeA). Scale bar, 125 μm.

(C) NkB is upregulated at 2 hr in the amygdala after fear conditioning. **p ≤ 0.01 versus home cage, n = 6–8 per group.

(D) Amygdala cell culture with osanetant, a potent and specific neurokinin 3 receptor (Nk3R) antagonist. Incubation with 20 μg and 40 μg of osanetant enhances *Nk3R* mRNA levels. This suggests that osanetant activates Nk3R and its downstream signaling in the amygdala. *p ≤ 0.05 versus Veh, **p ≤ 0.01 versus Veh, n = 2 per group. Mean + SEM is shown.

(Figure 2G) may provide deeper understanding of the functions of gamma-aminobutyric acid (GABA) in fear learning. Calmodulin-Dependent Protein Kinase II α (CaMKIIα), a well-characterized neuronal population involved in synaptic plasticity, is also colocalized with *Tac2* mRNA in the CeM (Figure 2H). Interestingly, GAD65 and CaMKII are associated with the consolidation of fear memories in the amygdala, although little is known about the specific role of these peptides in each substructure (Bergado-Acosta et al., 2008; Lepicard et al., 2006).

We also examined detection of the NkB peptide in amygdala cell culture, demonstrating that the peptide is highly present in both soma of neurons and dendrites (Figure 3A). Moreover, NkB peptide is also highly expressed in the CeA (Figure 3B). Interestingly, NkB is upregulated in the amygdala 2 hr after FC (Student's t test, $t = -2.902$, **p ≤ 0.01 fear conditioning versus home cage; Figure 3C). The Nk3R antagonist osanetant has already been used in humans in clinical trials for schizophrenia. Although it appears to have no beneficial effects in the treatment of schizophrenia, these studies show that it is well tolerated and safe in humans (Meltzer et al., 2004). Here, in amygdala cell culture, osanetant inactivates the Nk3R and leads to a compensatory increase in Nk3R expression as suggested by dose-dependent enhanced *Nk3R* mRNA levels (ANOVA $F_{3,5} = 10.014$, p ≤ 0.05; post hoc *p ≤ 0.05 versus Vehicle (Veh), **p ≤ 0.01 versus Veh; Figure 3D).

Osanetant and Emotional Learning

The above studies suggest that osanetant may be an ideal candidate to target the Nk3R in the amygdala in vivo, and we wished to examine its effects behaviorally. Osanetant given systemically, 30 min before open-field, elevated plus maze, and the conditioning chamber elicits no changes in anxiety-like behavior, locomotor activity, or electric shock reactivity (Figure S4). Notably, when osanetant is dosed from 30 min before auditory FC up to 1 hr after training, it does not affect fear acquisition but impairs fear memory consolidation as shown by decreased freezing in the fear expression test (Figures 4A and S4G; Student's t test, 30 min, $t = 3.042$; 10 min after FC, $t = 2.277$; 1 hr after FC, $t = 2.872$; *p ≤ 0.05 versus vehicle).

Recently, the PACAP-PAC1R pathway has been associated with PTSD in humans as well as in animal models (Ressler et al., 2011; Stevens et al., 2014). These prior data showed that expression of the *ADCYAP1R1* gene (encoding the PAC1 receptor) is increased following FC. Here we found that osanetant given before FC also normalizes the levels of *ADCYAP1R1* mRNA levels in the amygdala (ANOVA $F_{2,31} = 5.541$, p ≤ 0.01; post hoc *p ≤ 0.05 versus Veh-FC; **p ≤ 0.01 versus Veh-FC; Figure 4B). These data suggest that inhibition of the *Tac2*/NKB/Nk3R pathway may prevent activation of a stress-related gene pathway previously associated with PTSD. Concordantly, bilateral infusion of osanetant in the CeA also impairs fear memory consolidation, suggesting that CeA-NK3R are required for the formation for emotional memories (Student's t test; $t = 2.268$, *p ≤ 0.05 versus vehicle; Figures 4C and 4D).

We have shown in previous studies that mice exposed for 2 hr to a severe one-time stressor, immobilization to a wooden board (IMO), present long-term PTSD-like symptoms: impaired fear extinction and spatial memory and enhanced anxiety-like behaviors (Andero et al., 2011, 2013). Additionally, IMO in rats elicits alterations of the hypothalamic-pituitary-adrenal (HPA) axis that may be similar to the process initiating PTSD in humans (Armario et al., 2008). Notably, *Tac2* mRNA levels were more robustly upregulated in IMO-treated mice than in naive mice after FC, consistent with enhanced *Tac2*-dependent fear processing (ANOVA $F_{3,53} = 6.242$, p ≤ 0.001, post hoc *p ≤ 0.05 versus HC, **p ≤ 0.01 versus IMO; Figure 4F). Additionally, osanetant given systemically after FC impaired memory consolidation in IMO-treated mice, as shown by decreased freezing in the fear expression test (ANOVA repeated-measures, $F_{1,13} = 6.072$, *p ≤ 0.05; Figure 4G). This suggests that Nk3R antagonism reduces enhanced fear memory consolidation in a PTSD-like model.

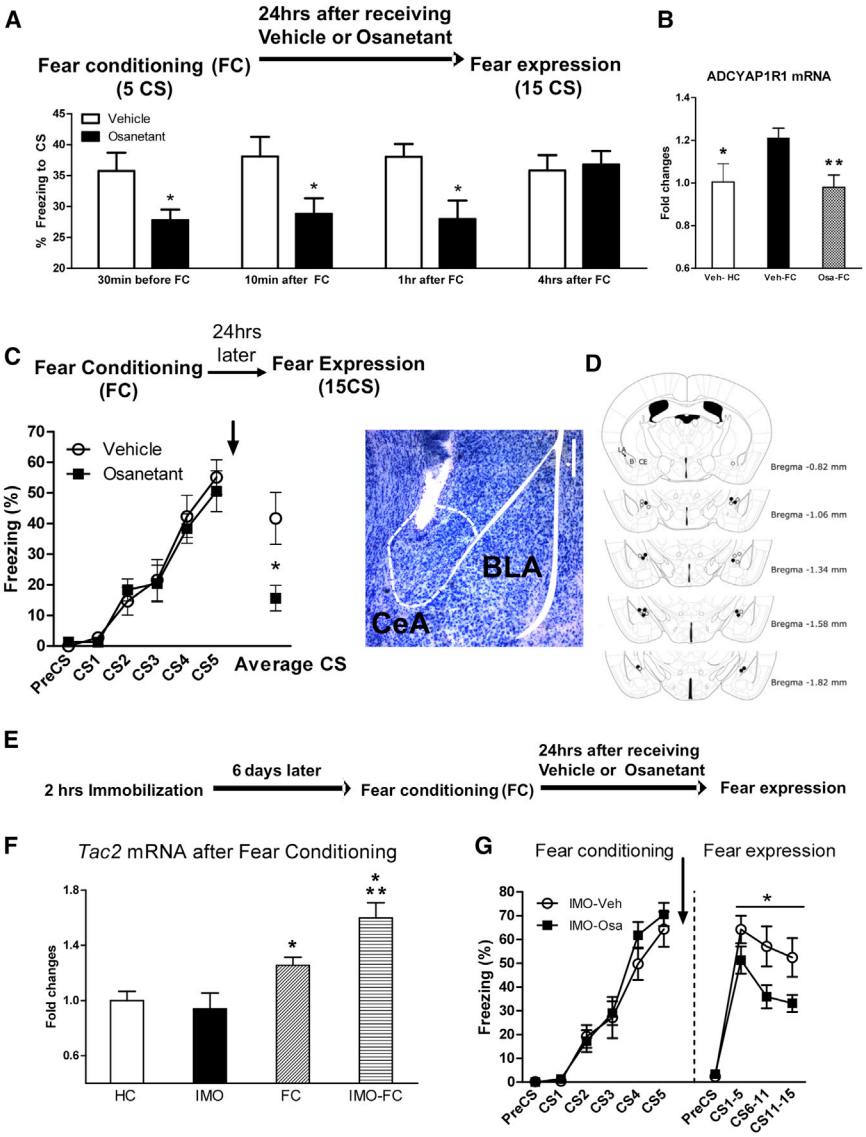

Figure 4. An Nk3R Antagonist Impairs Cued-Fear Memory Consolidation when Infused Systemically in the Central Amygdala and in a PTSD-like Mouse Model

(A) Osanetant impairs cued-fear memory when given from 30 min to up to 1 hr after fear acquisition. The figure shows the time spent in freezing behavior during the fear expression test when the CS is presented. *p ≤ 0.05 versus Veh. n = 4–12 per group.

(B) Osanetant given intraperitoneally 30 min before fear conditioning impaired the enhancement of mRNA levels of the Pac1 receptor (*Adcyap1r1*), *p ≤ 0.05 versus Veh-FC; **p ≤ 0.01 versus Veh-FC. n = 9–12 per group. The PACAP-PAC1R pathway is associated with PTSD, fear conditioning, and stress.

(C) Osanetant bilaterally injected into the central amygdala immediately after fear conditioning causes impaired fear memory consolidation as shown by lower freezing in the cued-fear expression test *p ≤ 0.05, n = 3–9 mice per group.

(D) Histological verification of osanetant infusion sites. Left: toluidine blue staining showing an example of the tip of the cannula in the CeA. Scale bar, 250 μm. Right: the dots indicate the lowest point of the injector tip.

(E) Timeline of the experiment.

(F) Cued-fear conditioning enhances *Tac2* levels 30 min after fear conditioning in naive mice but more robustly in mice with a previous exposure to immobilization to a wooden board (IMO), a PTSD-like model. n = 12–15 per group. *p ≤ 0.05 versus HC, **p ≤ 0.01 versus IMO.

(G) Osanetant was given immediately after FC and impaired fear memory consolidation in mice that had been previously exposed to a traumatic stress as shown by reduced freezing in the fear expression test, *p ≤ 0.05. n = 8 per group. Mean + or ± SEM is shown. Veh, vehicle; Osa, osanetant.

Tac2 Overexpression and Blockade by Osanetant

We next developed a viral vector to overexpress the *Tac2* gene in an inducible fashion within the brain, the lentivirus-*Tac2* (LV-*Tac2*). We first tested its functional expression by infecting HEK293 cells with the LV-*Tac2* compared to control LV-GFP lentiviruses, demonstrating that the NkB peptide was robustly expressed (Figures 5A and 5B). We then examined the behavioral effects of *Tac2* overexpression in mice. LV-*Tac2* or LV-GFP were bilaterally infused in the CeA (Figures 5C and 5D) and 14 days later *Tac2* was found to be overexpressed by 42%, as determined by mRNA levels with in situ hybridization, compared to mice that had received LV-GFP (Student's t test; $t = -3.841$, ***p ≤ 0.001 versus LV-GFP; Figure 5E). Mice infected with the LV-*Tac2* or LV-GFP received systemic osanetant or vehicle immediately after FC, and then fear expression was tested 24 hr later. Specific CeA-*Tac2* overexpression elicited a significant enhancement of fear memory consolidation (ANOVA $F_{3,20} = 8.512$, p ≤ 0.05; post hoc **p ≤ 0.01 versus LV-GFP-Veh; Figure 5H, right). Interestingly, we found that *Tac2* overexpression in the CeA did not induce changes in anxiety-like behavior or fear acquisition (Figures 5G and 5H). Replicating our previous findings, osanetant impaired fear memory consolidation when given to mice with the control LV-GFP (post hoc, *p ≤ 0.05 versus LV-GFP-Veh; Figure 5H, right). Additionally, the enhanced fear memory consolidation caused by CeA-*Tac2* overexpression was reversed by osanetant (post hoc, **p ≤ 0.01 versus LV-*Tac2*-Osa and LV-GFP-Osa; Figure 5H, right). See Figure S5 for a graphical representation of the *Tac2*-LV overexpression.

Silencing of *Tac2*-Expressing Cells and Emotional Learning

To further understand the role of the *Tac2* gene, we temporarily silenced the activity of neurons expressing this gene in the CeA during fear learning using designer receptors exclusively activated by designer drugs (DREADD) technology. The B6.129-*Tac2*tm1.1(cre)Qima/J (*Tac2*-Cre) (Mar et al., 2012) mice were

infected with a DREADD Gi-coupled receptor via the pAAV-hSyn double-floxed hM4D-mCherry virus (hM4Di-mCherry AAV) (Figure 6A). This elicited specific expression of the mCherry reporter in *Tac2* cells within the CeA, but not any other area of the brain, suggesting the insertion of the DREADD receptor on the plasma membrane (Figures 6B and 6C; Krashes et al., 2011). Fourteen days later, clozapine-N-oxide (CNO), which binds to the inserted receptor but otherwise is pharmacologically inert, was given systemically 30 min before FC in both groups, *Tac2*-Cre-/hM4Di-mCherry and *Tac2*-Cre+/hM4Di-mCherry. CNO had no effect on fear acquisition as shown by equivalent amount of freezing in both groups (Figure 6D). However, when animals were tested for fear expression, 24 hr later in the absence of CNO, the *Tac2*-Cre+/hM4Di-mCherry mice presented less freezing, suggesting impaired fear memory consolidation (Student's t test, $t = 3.257$, $^{*}p \leq 0.05$ *Tac2*-Cre-/hM4Di-mCherry versus *Tac2*-Cre+/hM4Di-mCherry; Figure 6D). This demonstrates that the animals expressing *Tac2*-Cre+/hM4Di-mCherry and inducible Gi to temporally silence the activity of *Tac2*-expressing neurons exhibit significantly less fear consolidation when tested for fear learning. Mice were then retrained with a different CS and a different context in the same FC apparatus, as in previous experiments but without dosing CNO. *Tac2*-Cre-/hM4Di-mCherry and *Tac2*-Cre+/hM4Di-mCherry mice showed similar amount of freezing in the FC and fear expression test (Figure 6E). This suggests that when *Tac2*-expressing neurons are not silenced, there is normal fear memory consolidation in both *Tac2*-Cre-/hM4Di-mCherry and *Tac2*-Cre+/hM4Di-mCherry groups. Moreover, when given CNO, these two groups presented equivalent levels of anxiety-like behavior and pain sensitivity (Figure 6F and Figure S6).

DISCUSSION

Previous reports have shown that Nk3R is associated with memory processes in hippocampus-dependent tasks in rodents (de Souza Silva et al., 2013; Siuciak et al., 2007; Zlomuzica et al., 2008). Here, we provide evidence that *Tac2*-NkB-Nk3R signaling within the CeA is required for the modulation of fear memory consolidation. Other studies have shown that the CeA is required for the acquisition, consolidation, and expression of fear memories (Wilensky et al., 2006). Here we show mechanisms that may also be involved in those processes within the CeA. To the best of our knowledge, this is the first evidence that a neuronal population specifically highly expressed in the CeM, *Tac2* and its product NkB peptide, are required for the modulation of fear memory consolidation affecting neither unconditioned fear nor anxiety-like behavior. All that is known about NkB release is from in vitro experiments, where it is suggested that NkB release is potassium evoked and calcium dependent, fulfilling the criterion of a neurotransmitter or a neuromodulator (Lindefors et al., 1985). More studies about this topic would be desirable to further understand the mechanisms of the *Tac2*/NkB/Nk3R pathway.

Our findings also suggest that CeA-*Tac2* lentiviral overexpression enhances fear memory consolidation but Nk3R antagonism prevents it. This shows that Nk3R antagonism within the CeA is able to normalize dysregulated functioning induced by the *Tac2* gene. We believe that it is possible that osanetant given systemically or intracranially within the CeA may be acting in the Nk3R in all areas of CeA and not only in the CeM (Smith and Flynn, 2000; Yip and Chahl, 1997). This impairment of fear memory consolidation by Nk3R antagonism is consistent with previous reports where Nk3R activation with senktide in the hippocampus and cortex leads to enhanced postsynaptic depolarization and long-term potentiation (LTP) in slice physiology studies, and this effect was blocked by NK3R antagonism (Gallopin et al., 2006; Rekling, 2004). However, specific electrophysiological experiments in the amygdala should be performed in the future to study whether activation or blockade of the Nk3R in this structure is involved in LTP or other types of activity-dependent plasticity.

In agreement with these prior findings, specific and temporal pharmacogenetic silencing of *Tac2*-expressing neurons in the CeA with DREADDs leads to impaired fear memory consolidation. Of note, no effects in fear acquisition, pain sensitivity, or anxiety-like behavior were detected when overexpressing *Tac2*, inhibiting *Tac2*-expressing neurons, or with the Nk3R antagonist, which is consistent with previous findings suggesting that the *Tac2*-NkB-Nk3R pathway is not directly involved in these processes, although it may modulate them (Ebner et al., 2009; Mar et al., 2012; Siuciak et al., 2007). Interestingly, in our fear paradigm, the *Tac2* gene within the amygdala is involved in auditory (CS+US paired) but not stress or contextual memories (US only). However, this does not preclude the hypothesis that different fear paradigms might reveal a role of *Tac2* in the amygdala in contextual fear conditioning.

Thus, we believe that enhanced *Tac2* gene expression in our fear models enhanced NkB production in the amygdala, binding to Nk3R and promoting fear memory consolidation. This upregulation of *Tac2* mRNA levels primarily within the CeM suggests several possible nonmutually exclusive scenarios. The first is that the *Tac2* gene synthesizes NkB in the CeM amygdala, acting on local Nk3R within the CeM specifically. The second is that *Tac2* mRNA and/or NkB are transported from the CeM to other nuclei within the amygdala such as CeL, CeC, or BLA, where they bind to the Nk3R. Our data also suggest that amygdala cell culture with osanetant increases *Nk3R* mRNA levels. The most likely interpretation is that osanetant antagonizes amygdala Nk3R and due to its decreased availability, *Nk3R* mRNA is increased to synthesize more Nk3R in a compensatory manner. The current data provide intriguing support for a specific role of *Tac2* gene, via NkB activation of Nk3R in fear consolidation within the CeA.

CeLon neurons essentially serve as disinhibitory cells for CeLoff neurons. Both CeLon and CeLoff neurons release GABA when activated. CeLon neurons send projections to CeLoff neurons, and, therefore, the increased firing of CeLon neurons during CS presentation results in inhibition of CeLoff neurons (normally inhibiting the CeM) and, thus, in disinhibition of CeM, promoting conditioned fear responses (Ciocchi et al., 2010). Specifically, CeLoff neurons largely overlap with PKCd+ neurons (Haubensak et al., 2010). Moreover, we also show that *Tac2* gene is not colocalized with *Enk* in the CeM. *Enk* is colocalized with *PKCd* in the CeL (Haubensak et al., 2010) and specific CeA-*Enk* deletion decreases fear expression during FC without

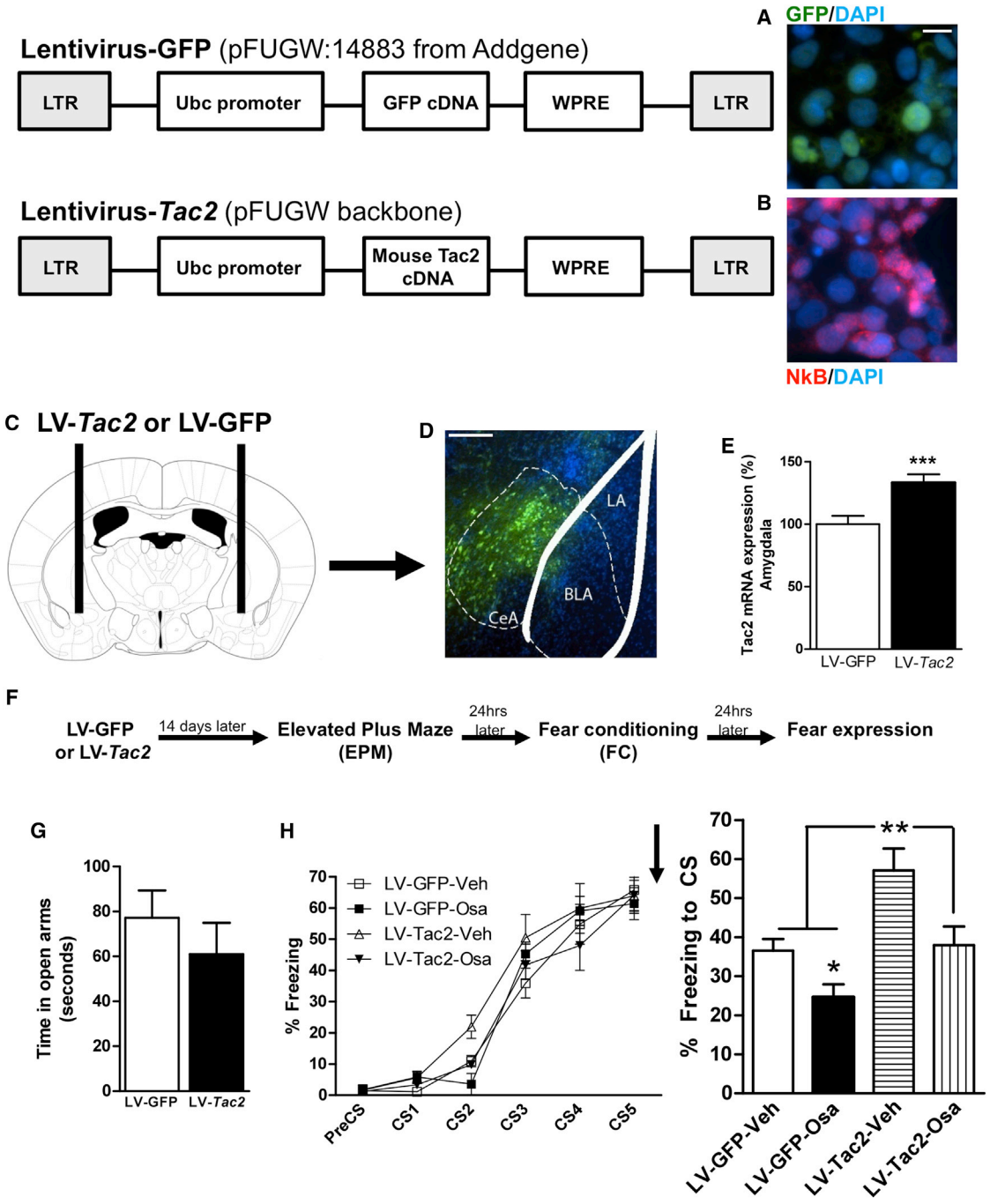

Figure 5. *Tac2* Overexpression in the Central Amygdala Is Sufficient to Enhance Fear Memory Consolidation and It Is Blocked by an Nk3R Antagonist

(A) The lentivirus GFP-FUGW induces GFP expression but not Neurokinin B (NkB) in Hek293 cells. Scale bar, 10 μm.

(B) The lentivirus *Tac2*-FUGW induces NkB expression in Hek293 cells. DAPI staining (blue) indicates the cellular nuclei. NkB staining (red) is contrasted with GFP fluorescence (green).

(C) *Tac2*-FUGW or GFP-FUGW was bilaterally infused in the central amygdala and mice were left undisturbed for 14 days.

(D) The lentivius *Tac2*-FUGW showing GFP expression in the CeA neurons infected with virus. Scale bar, 250 μm.

(E) Lentivirus *Tac2*-FUGW expression causes a 42% overexpression of *Tac2* in the central amygdala. ***p ≤ 0.001 versus LV-GFP. n = 9–15 per group.

(F) Timeline of the experiment.

(legend continued on next page)

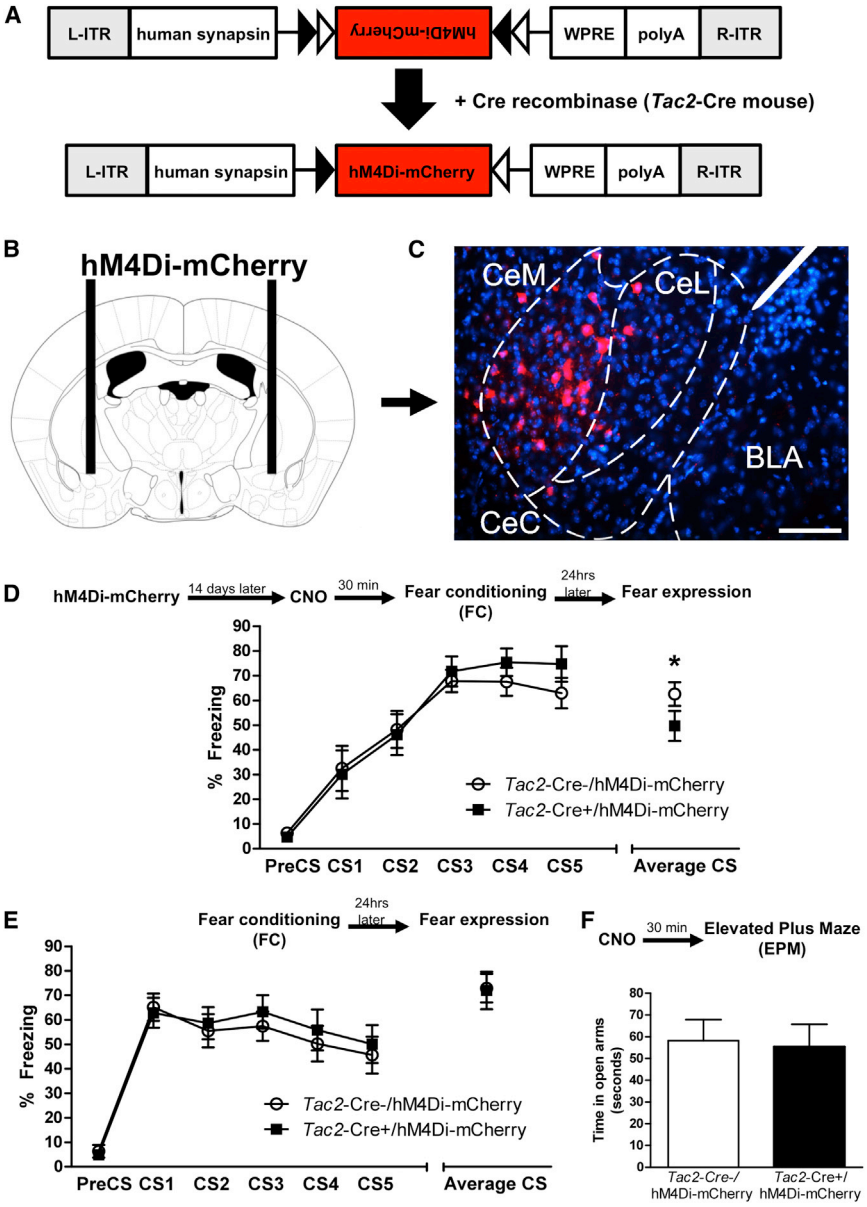

Figure 6. Inducible Silencing of *Tac2*-Expressing Neurons in the CeA with Gi-DREADD Decreases Conditioned Fear

(A) Design of hM4Di-mCherry AAV and *Tac2*-Cre mice.

(B) *Tac2*-Cre- or *Tac2*-Cre+ mice were infected with the hM4Di-mCherry AAV in the CeA.

(C) The Gi receptor was inserted only on the *Tac2*-Cre cells of *Tac2*-Cre+ mice as shown with mCherry expression from infected CeA; CeM, centromedial amygdala; CeL, centrolateral amygdala; BLA, basolateral amygdala. Scale bar, 125 μm.

(D) CNO was given systemically 30 min prior to fear conditioning to *Tac2*-Cre-/hM4Di-mCherry and *Tac2*-Cre+/hM4Di-mCherry mice. Temporal silencing of the *Tac2*-expressing neurons in the *Tac2*-Cre+/hM4Di-mCherry group did not affect freezing during fear acquisition. However, when mice were tested the day after for fear expression, without CNO, *Tac2*-Cre+/hM4Di-mCherry mice showed less conditioned fear. *$p \leq 0.05$ *Tac2*-Cre-/hM4Di-mCherry versus *Tac2*-Cre+/hM4Di-mCherry, n = 10–11 per group.

(E) *Tac2*-Cre-/hM4Di-mCherry and *Tac2*-Cre+/hM4Di-mCherry mice were retrained to a different acoustic tone (CS) without receiving CNO. Both groups equally acquired fear learning and showed similar levels of fear memory consolidation.

(F) CNO given 30 min before the elevated plus maze showed no effect on *Tac2*-Cre-/hM4Di-mCherry or *Tac2*-Cre+/hM4Di-mCherry in anxiety-like behavior. See also Figure S6.

affecting fear memory consolidation (Poulin et al., 2013). Thus, the *Tac2*-CeM neuronal population appears to be independent of, and complementary to, other previously described neuronal populations involved in FC. The GAD65 peptide, abundantly found at nerve terminals and synapses, plays a key role in GABA neurotransmission (Pinal and Tobin, 1998). Additionally, CaMKII is a well-known marker for synaptic plasticity. Thus, the colocalization of *Tac2* mRNA levels and GAD65 and CaMKIIα peptides in the CeM suggest that *Tac2* gene may have a role in neurotransmission within the GAD65 and CaMKIIα-expressing neurons, in agreement with our data that suggest that this CeM population may be critically involved in fear memory consolidation.

Finally, one of the most interesting aspects of our data is the potential use of the Nk3R antagonist osanetant as a pharmacological agent to block fear memory consolidation shortly after exposure to a trauma. Additionally, we found that osanetant prevented the upregulation of the *Adcyap1r1* gene, which encodes the PAC1 receptor. The PACAP-PAC1R pathway is involved in PTSD, fear conditioning, amygdala excitatory neurotransmission, and stress (Almli et al., 2013; Cho et al., 2012; Hashimoto et al., 2011; Ressler et al., 2011; Uddin et al., 2013). All this could be relevant in PTSD prevention since it has previously been found that osanetant is safe in humans, although additional preclinical studies, such as those described herein, are needed first to establish the mechanisms involved. This gives our findings an exciting potential approach

(G) *Tac2* overexpression in the central amygdala does not alter anxiety-like behavior evaluated by the time spent in the open arms in the elevated plus maze. n = 9–15.

(H) Left: the lentiviruses GFP-FUGW and *Tac2*-FUGW cause no changes in fear conditioning. Osanetant or vehicle were given systemically immediately after fear acquisition. Right: *Tac2* overexpression enhances fear memory consolidation (LV-*Tac2*-Veh) and osanetant impairs this effect (LV-*Tac2*-Osa). n = 3–8 per group. *$p \leq 0.05$ versus LV-GFP-Veh, **$p \leq 0.01$ versus all other groups. Mean + or ± SEM is shown. See also Figure S5.

to translation to human patients. Although other molecular pathways have previously been associated with PTSD, we believe that there will be a number of different mechanisms identified that eventually will synergistically be used to target emotional memory modulation.

In summary, these studies provide understanding of the role of the *Tac2* gene and the CeM in fear processing and provide approaches to intervention for fear-related disorders.

EXPERIMENTAL PROCEDURES

Procedures are described in detail in Supplemental Experimental Procedures.

Mice

Amygdala cell culture experiments were performed with male wild-type (WT) C57BL/6J p21 mice. All other experiments were performed on adult WT C57BL/6J or B6.129-*Tac2*tm1.1(cre)Qima/J (*Tac2*-Cre) (Mar et al., 2012) from Jackson Laboratory (Stock 018938), male mice that were group-housed in a temperature-controlled vivarium, with ad libitum access to food and water. Animals were maintained on a 12 hr/12 hr light/dark cycle, with all behavioral procedures being performed during the light cycle. All procedures used were approved by the Institutional Animal Care and Use Committee of Emory University and in compliance with National Institutes of Health (NIH) Guide for the Care and Use of Laboratory Animals.

Immobilization to Wooden Board

Mice were exposed once for 2 hr to IMO, which was performed as previously described (Andero et al., 2011, 2013).

mRNA Extraction and Microarray

Total mRNA was isolated and purified from the tissue with the RNeasy Mini Kit (catalog 74106, QIAGEN). Illumina MouseWG-6 v2 Expression BeadChip microarray (Illumina) was assayed for 45,281 transcripts as previously described (Andero et al., 2013). FDR was calculated with SAM 4.01 using a 5% cutoff for the FDR rate. The heat maps were created with Genesis 1.4.0 (Sturn et al., 2002). The pathway analysis was generated through the use of IPA (Ingenuity Systems, http://www.ingenuity.com). The microarray data are publicly available in the Gene Expression Omnibus database under accession number GSE57465.

Behavioral Experiments

Elevated plus-maze, open-field, cued-fear conditioning, and fear expression tests were performed as previously described (Andero et al., 2011, 2013). The CS was 30 s 0.6 kHz tone and the US was 1 mA 500 ms electric footshocks. Retraining of mice was performed with a 12 kHz tone.

Complementary DNA Synthesis and qPCR

Total mRNA was reverse transcribed with the RT^2 First Strand Kit (catalog 330401, QIAGEN). The primers used for the qPCR were TaqMan *Tac2* Mm01160362_m1, *ADCYAP1R1* Mm01326453_m1, and *NK3R* Mm00445346_m1 from Applied Biosystems. The qPCR was performed and analyzed as previously described (Andero et al., 2013).

Radioactive In Situ Hybridization

Tissue was fixed in 4% paraformaldehyde, pretreated, and hybridized with 36SUTP-labeled cRNA riboprobes prepared from linearized constructs for antisense sequence of *Tac2* (T7 RNA polymerase) as previously described (Rattiner et al., 2004).

Fluorescent In Situ Hybridization

cRNA riboprobes were prepared from linearized constructs for antisense sequences of *Tac2*, *PKCd*, and *Enkephalin* (T7 RNA polymerase) as previously described (Jasnow et al., 2013). The *Tac2* riboprobe was labeled with fluorescein and the *PKCd* and *Enkephalin* with digoxigenin. Signals were amplified with the TSA Plus Fluorescein Fluorescence System or TSA Plus Cy5 Fluorescence System (PerkinElmer) following each series of primary antibodies. Sections were then stained with DAPI (1:1,000), washed, and coverslipped with Mowiol mounting medium (Jasnow et al., 2013).

Amygdala Cell Culture

Amygdala primary cell culture was performed as previously described (Mou et al., 2011).

Immunohistochemistry

Pep2/ProNkB, IS-39 ab (1:500) was the antibody used to detect NkB. The procedure was followed as previously described (Kalló et al., 2012). The procedure for detecting Gad65 (AB5082, Chemicon, 1:500) and CaMkIIα (Cell Signaling Solutions, 1:250) was similar as previously described (Jasnow et al., 2013) after performing the *Tac2* FISH. After the ISH and IHC sections were stained with DAPI (1:1,000), they were washed and coverslipped with Mowiol mounting medium.

Immunocytochemistry

Immunocytochemistry was performed as previously described (Mou et al., 2011). The antibody used was Pep2/ProNkB IHC (IS-39 ab, 1:500) (Kalló et al., 2012) and DAPI or NeuN (1:1,000).

ELISA

The mouse Neurokinin B ELISA kit was purchased from Mybiosource (Catalogue MBS744693). The inter-assay coefficient of variation is 7.5%–8.6%, the intra-assay coefficient of variation is 8.2%–9.5% and the spike recovery is 95%–103%. Procedure was followed as indicated by the manufacturer.

Production of Recombinant Viral Vectors

Mixture for transfection was 250 ug of FUGW or FUW-*Tac2* + 187.5 ug of pCMVdelta 8.9 + 75 ug of pV-SVG + 12 ml of ddH2O + 12.5 ml of 0.5M Ca2Cl + 25 ml of 2× HeBS to total volume 50 ml; this solution was vortexed a few seconds and incubated for 20 min at room temperature. Procedure was followed as previously described (Huang et al., 2013). The pAAV-hSyn-double floxed hM4D-mCherry (hM4Di-mCherry AAV) was purchased from UNC Gene Therapy Center.

Surgery and Injection of Virus

Mice were anesthetized and placed in a stereotaxic frame. CeA coordinates were as follows: anteroposterior, −1.34 mm; dorsoventral, −4.4 mm; mediolateral, −2.4 mm relative to bregma. For the LV-*Tac2* experiments, the animals received bilateral intra-CeA amygdala injections of lentiviral vectors expressing *Tac2*-FUW or FUGW (GFP) in 1% BSA in PBS, 0.5 μl of virus/side. We injected 1 μl of virus/side of the pAAV-hSyn-double floxed hM4D-mCherry (hM4Di-mCherry AAV) in the CeA of *Tac2*-Cre- and *Tac2*-Cre+ mice. For all experiments, the rate of injection was 0.1 μl/min and the needle was left in place for 10 min after injection and the skin was closed using a 6-0 Vicryl suture.

Drug Administration

The Nk3R antagonist osanetant (Axon Medchem, Axon 1533) was dissolved in physiological saline and 0.1% Tween 20, which was also the vehicle. Intraperitoneal (i.p.) dose was 5 mg/kg for systemic administration and 0.5 μl with 625 ng dose per side for the intra-CeA studies. Cannulation of the mice was performed as previously described (Andero et al., 2013). Clozapine-N-oxide (CNO, Sigma Aldrich C0832) was given i.p. at 1 mg/kg (Krashes et al., 2011).

Statistics

Statistics were performed with IBM SPSS Statistics 19.0. Detection of outliers was performed and, when necessary, removed from analyses. ANOVA followed by post hoc analyses were appropriate, repeated-measures ANOVA, or Student's t test (two-tailed) for independent samples was tested. The results are presented as means ± or + SEM, and statistical significance was set at $p \leq 0.05$.

ACCESSION NUMBERS

The GEO accession number for the microarray data reported in this paper is GSE57465.

SUPPLEMENTAL INFORMATION

Supplemental Information includes Supplemental Experimental Procedures, six figures, and two tables and can be found with this article online at http://dx.doi.org/10.1016/j.neuron.2014.05.028.

ACKNOWLEDGMENTS

The authors would like to thank the following for their help: Greg Doho (Microarray, Emory Cancer Genomics Shared Resource), Xinping Huang (Lentivirus, Viral Vector Core, Emory University), Oskar Laur (Cloning, Custom Cloning Core Facility, Emory University), Noreen Khan and Robert Bruner (behavior), Liping Mou (cell culture), Georgette Gafford (ISH and FISH), Aaron Jasnow (ISH), Takehito Sawamura (stereotaxic surgery), Mallory Bowers and Joanna Dabrowska (confocal microscope), Dennis Choi (comments on the data), and Philippe Cioffi (donation of the NkB antibody IS-39). This research project was supported in part by the Viral Vector Core of the Emory Neuroscience NINDS Core Facilities grant, P30NS055077. This project was also funded by the Office of Research Infrastructure Programs/OD P51OD011132 (formerly NCRR P51RR000165). This work was also supported by these sources of funding: 1R21MH101492-01 (R.A. and K.J.R.) and 1R01MH096764 (K.J.R.), Burroughs Wellcome Fund and HHMI.

Accepted: May 9, 2014
Published: June 26, 2014

REFERENCES

Almli, L.M., Mercer, K.B., Kerley, K., Feng, H., Bradley, B., Conneely, K.N., and Ressler, K.J. (2013). ADCYAP1R1 genotype associates with post-traumatic stress symptoms in highly traumatized African-American females. Am. J. Med. Genet. B. Neuropsychiatr. Genet. *162B*, 262–272.

American Psychiatric Association (2013). Diagnostic and Statistical Manual of Mental Disorders, Fourth Edition, Text Revision (DSM5). (Washington, DC: American Psychiatric Publishing).

Andero, R., and Ressler, K.J. (2012). Fear extinction and BDNF: translating animal models of PTSD to the clinic. Genes Brain Behav. *11*, 503–512.

Andero, R., Heldt, S.A., Ye, K., Liu, X., Armario, A., and Ressler, K.J. (2011). Effect of 7,8-dihydroxyflavone, a small-molecule TrkB agonist, on emotional learning. Am. J. Psychiatry *168*, 163–172.

Andero, R., Brothers, S.P., Jovanovic, T., Chen, Y.T., Salah-Uddin, H., Cameron, M., Bannister, T.D., Almli, L., Stevens, J.S., Bradley, B., et al. (2013). Amygdala-dependent fear is regulated by Oprl1 in mice and humans with PTSD. Sci. Transl. Med. *5*, 88ra73.

Armario, A., Escorihuela, R.M., and Nadal, R. (2008). Long-term neuroendocrine and behavioural effects of a single exposure to stress in adult animals. Neurosci. Biobehav. Rev. *32*, 1121–1135.

Beaujouan, J.C., Torrens, Y., Saffroy, M., Kemel, M.L., and Glowinski, J. (2004). A 25 year adventure in the field of tachykinins. Peptides *25*, 339–357.

Bergado-Acosta, J.R., Sangha, S., Narayanan, R.T., Obata, K., Pape, H.C., and Stork, O. (2008). Critical role of the 65-kDa isoform of glutamic acid decarboxylase in consolidation and generalization of Pavlovian fear memory. Learn. Mem. *15*, 163–171.

Cho, J.H., Zushida, K., Shumyatsky, G.P., Carlezon, W.A., Jr., Meloni, E.G., and Bolshakov, V.Y. (2012). Pituitary adenylate cyclase-activating polypeptide induces postsynaptically expressed potentiation in the intra-amygdala circuit. J. Neurosci. *32*, 14165–14177.

Ciocchi, S., Herry, C., Grenier, F., Wolff, S.B., Letzkus, J.J., Vlachos, I., Ehrlich, I., Sprengel, R., Deisseroth, K., Stadler, M.B., et al. (2010). Encoding of conditioned fear in central amygdala inhibitory circuits. Nature *468*, 277–282.

de Souza Silva, M.A., Lenz, B., Rotter, A., Biermann, T., Peters, O., Ramirez, A., Jessen, F., Maier, W., Hüll, M., Schröder, J., et al. (2013). Neurokinin3 receptor as a target to predict and improve learning and memory in the aged organism. Proc. Natl. Acad. Sci. USA *110*, 15097–15102.

Duarte, C.R., Schütz, B., and Zimmer, A. (2006). Incongruent pattern of neurokinin B expression in rat and mouse brains. Cell Tissue Res. *323*, 43–51.

Dunlop, B.W., Mansson, E., and Gerardi, M. (2012). Pharmacological innovations for posttraumatic stress disorder and medication- enhanced psychotherapy. Curr. Pharm. Des. *18*, 5645–5658.

Ebner, K., Sartori, S.B., and Singewald, N. (2009). Tachykinin receptors as therapeutic targets in stress-related disorders. Curr. Pharm. Des. *15*, 1647–1674.

Gallopin, T., Geoffroy, H., Rossier, J., and Lambolez, B. (2006). Cortical sources of CRF, NKB, and CCK and their effects on pyramidal cells in the neocortex. Cereb. Cortex *16*, 1440–1452.

Gether, U. (2000). Uncovering molecular mechanisms involved in activation of G protein-coupled receptors. Endocr. Rev. *21*, 90–113.

Hashimoto, H., Shintani, N., Tanida, M., Hayata, A., Hashimoto, R., and Baba, A. (2011). PACAP is implicated in the stress axes. Curr. Pharm. Des. *17*, 985–989.

Haubensak, W., Kunwar, P.S., Cai, H., Ciocchi, S., Wall, N.R., Ponnusamy, R., Biag, J., Dong, H.W., Deisseroth, K., Callaway, E.M., et al. (2010). Genetic dissection of an amygdala microcircuit that gates conditioned fear. Nature *468*, 270–276.

Hetrick, S.E., Purcell, R., Garner, B., and Parslow, R. (2010). Combined pharmacotherapy and psychological therapies for post traumatic stress disorder (PTSD). Cochrane Database Syst. Rev. CD007316.

Huang, X., Hartley, A.V., Yin, Y., Herskowitz, J.H., Lah, J.J., and Ressler, K.J. (2013). AAV2 production with optimized N/P ratio and PEI-mediated transfection results in low toxicity and high titer for in vitro and in vivo applications. J. Virol. Methods *193*, 270–277.

Jasnow, A.M., Ehrlich, D.E., Choi, D.C., Dabrowska, J., Bowers, M.E., McCullough, K.M., Rainnie, D.G., and Ressler, K.J. (2013). Thy1-expressing neurons in the basolateral amygdala may mediate fear inhibition. J. Neurosci. *33*, 10396–10404.

Kalló, I., Vida, B., Deli, L., Molnár, C.S., Hrabovszky, E., Caraty, A., Ciofi, P., Coen, C.W., and Liposits, Z. (2012). Co-localisation of kisspeptin with galanin or neurokinin B in afferents to mouse GnRH neurones. J. Neuroendocrinol. *24*, 464–476.

Kearns, M.C., Ressler, K.J., Zatzick, D., and Rothbaum, B.O. (2012). Early interventions for PTSD: a review. Depress. Anxiety *29*, 833–842.

Khawaja, A.M., and Rogers, D.F. (1996). Tachykinins: receptor to effector. Int. J. Biochem. Cell Biol. *28*, 721–738.

Krashes, M.J., Koda, S., Ye, C., Rogan, S.C., Adams, A.C., Cusher, D.S., Maratos-Flier, E., Roth, B.L., and Lowell, B.B. (2011). Rapid, reversible activation of AgRP neurons drives feeding behavior in mice. J. Clin. Invest. *121*, 1424–1428.

Lepicard, E.M., Mizuno, K., Antunes-Martins, A., von Hertzen, L.S., and Giese, K.P. (2006). An endogenous inhibitor of calcium/calmodulin-dependent kinase II is up-regulated during consolidation of fear memory. Eur. J. Neurosci. *23*, 3063–3070.

Lindefors, N., Brodin, E., Theodorsson-Norheim, E., and Ungerstedt, U. (1985). Calcium-dependent potassium-stimulated release of neurokinin A and neurokinin B from rat brain regions in vitro. Neuropeptides *6*, 453–461.

Mar, L., Yang, F.C., and Ma, Q. (2012). Genetic marking and characterization of Tac2-expressing neurons in the central and peripheral nervous system. Mol. Brain *5*, 3.

Meltzer, H.Y., Arvanitis, L., Bauer, D., and Rein, W.; Meta-Trial Study Group (2004). Placebo-controlled evaluation of four novel compounds for the treatment of schizophrenia and schizoaffective disorder. Am. J. Psychiatry *161*, 975–984.

Mileusnic, D., Lee, J.M., Magnuson, D.J., Hejna, M.J., Krause, J.E., Lorens, J.B., and Lorens, S.A. (1999). Neurokinin-3 receptor distribution in rat and human brain: an immunohistochemical study. Neuroscience *89*, 1269–1290.

Mou, L., Heldt, S.A., and Ressler, K.J. (2011). Rapid brain-derived neurotrophic factor-dependent sequestration of amygdala and hippocampal GABA(A) receptors via different tyrosine receptor kinase B-mediated phosphorylation pathways. Neuroscience *176*, 72–85.

Nagano, M., Saitow, F., Haneda, E., Konishi, S., Hayashi, M., and Suzuki, H. (2006). Distribution and pharmacological characterization of primate NK-1 and NK-3 tachykinin receptors in the central nervous system of the rhesus monkey. Br. J. Pharmacol. *147*, 316–323.

Norrholm, S.D., and Ressler, K.J. (2009). Genetics of anxiety and trauma-related disorders. Neuroscience *164*, 272–287.

Petrovich, G.D., Scicli, A.P., Thompson, R.F., and Swanson, L.W. (2000). Associative fear conditioning of enkephalin mRNA levels in central amygdalar neurons. Behav. Neurosci. *114*, 681–686.

Pinal, C.S., and Tobin, A.J. (1998). Uniqueness and redundancy in GABA production. Perspect. Dev. Neurobiol. *5*, 109–118.

Poulin, J.F., Bérubé, P., Laforest, S., and Drolet, G. (2013). Enkephalin knockdown in the central amygdala nucleus reduces unconditioned fear and anxiety. Eur. J. Neurosci. *37*, 1357–1367.

Rattiner, L.M., Davis, M., and Ressler, K.J. (2004). Differential regulation of brain-derived neurotrophic factor transcripts during the consolidation of fear learning. Learn. Mem. *11*, 727–731.

Rekling, J.C. (2004). NK-3 receptor activation depolarizes and induces an after-depolarization in pyramidal neurons in gerbil cingulate cortex. Brain Res. Bull. *63*, 85–90.

Ressler, K.J., Paschall, G., Zhou, X.L., and Davis, M. (2002). Regulation of synaptic plasticity genes during consolidation of fear conditioning. J. Neurosci. *22*, 7892–7902.

Ressler, K.J., Mercer, K.B., Bradley, B., Jovanovic, T., Mahan, A., Kerley, K., Norrholm, S.D., Kilaru, V., Smith, A.K., Myers, A.J., et al. (2011). Post-traumatic stress disorder is associated with PACAP and the PAC1 receptor. Nature *470*, 492–497.

Siuciak, J.A., McCarthy, S.A., Martin, A.N., Chapin, D.S., Stock, J., Nadeau, D.M., Kantesaria, S., Bryce-Pritt, D., and McLean, S. (2007). Disruption of the neurokinin-3 receptor (NK3) in mice leads to cognitive deficits. Psychopharmacology (Berl.) *194*, 185–195.

Smith, M.E., and Flynn, F.W. (2000). Distribution of Fos-like immunoreactivity within the rat brain following intraventricular injection of the selective NK(3) receptor agonist senktide. J. Comp. Neurol. *426*, 413–428.

Stevens, J.S., Almli, L.M., Fani, N., Gutman, D.A., Bradley, B., Norrholm, S.D., Reiser, E., Ely, T.D., Dhanani, R., Glover, E.M., et al. (2014). PACAP receptor gene polymorphism impacts fear responses in the amygdala and hippocampus. Proc. Natl. Acad. Sci. USA *111*, 3158–3163.

Sturn, A., Quackenbush, J., and Trajanoski, Z. (2002). Genesis: cluster analysis of microarray data. Bioinformatics *18*, 207–208.

Uddin, M., Chang, S.C., Zhang, C., Ressler, K., Mercer, K.B., Galea, S., Keyes, K.M., McLaughlin, K.A., Wildman, D.E., Aiello, A.E., and Koenen, K.C. (2013). Adcyap1r1 genotype, posttraumatic stress disorder, and depression among women exposed to childhood maltreatment. Depress. Anxiety *30*, 251–258.

Vermetten, E., and Lanius, R.A. (2012). Biological and clinical framework for posttraumatic stress disorder. Handb. Clin. Neurol. *106*, 291–342.

Wilensky, A.E., Schafe, G.E., Kristensen, M.P., and LeDoux, J.E. (2006). Rethinking the fear circuit: the central nucleus of the amygdala is required for the acquisition, consolidation, and expression of Pavlovian fear conditioning. J. Neurosci. *26*, 12387–12396.

Yip, J., and Chahl, L.A. (1997). Localization of Fos-like immunoreactivity induced by the NK3 tachykinin receptor agonist, senktide, in the guinea-pig brain. Br. J. Pharmacol. *122*, 715–725.

Zlomuzica, A., Dere, E., Huston, J.P., and de Souza Silva, M.A. (2008). NK(3) receptor agonism promotes episodic-like memory in mice. Neurobiol. Learn. Mem. *90*, 420–425.

Neuron, Volume *83*

Supplemental Information

A Role for *Tac2,* NkB, and Nk3 Receptor in Normal and Dysregulated Fear Memory Consolidation

Raül Andero, Brian G. Dias, and Kerry J. Ressler

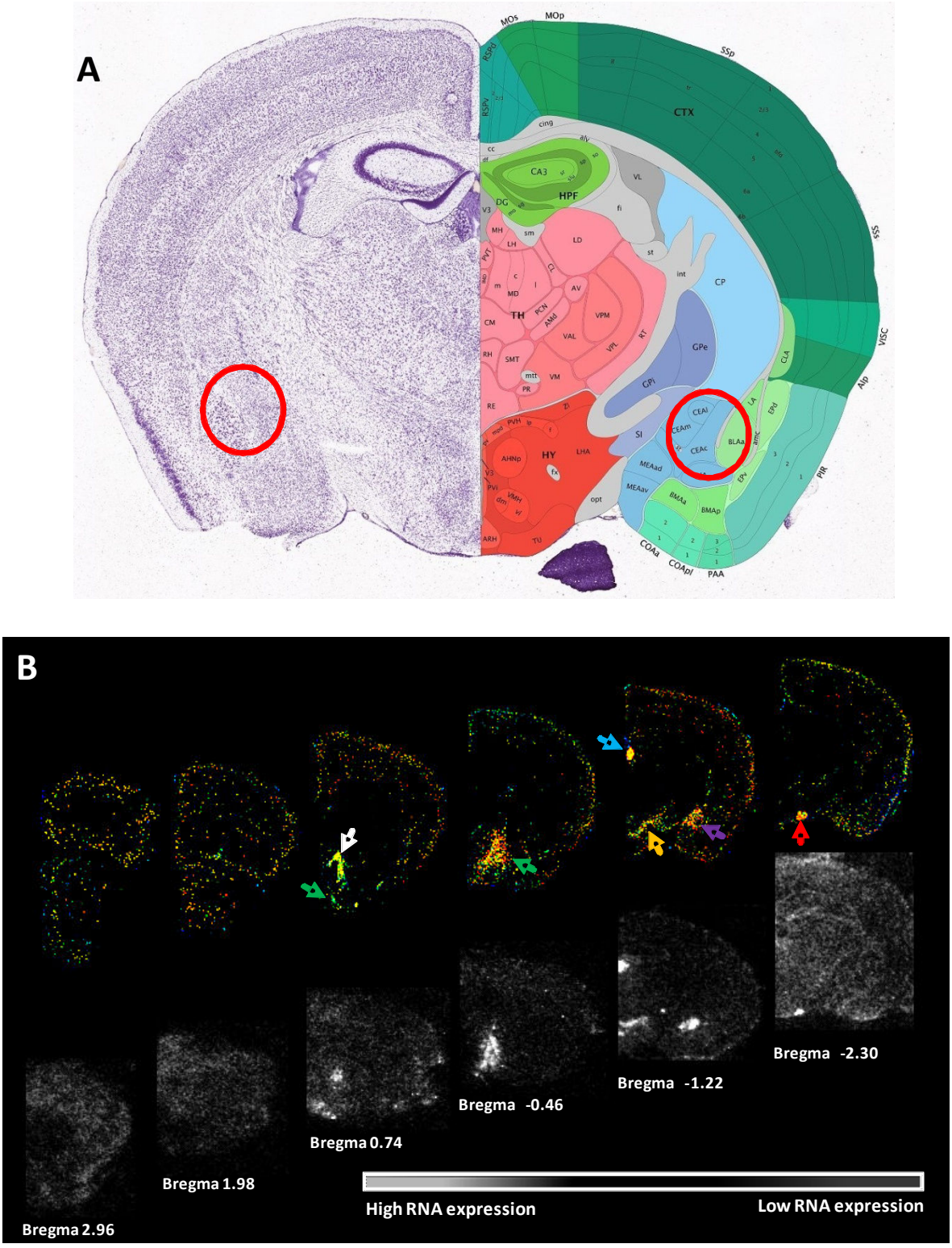

Figure S1, related to Figure 1. Amygdala micropunches and *Tac2* in the adult male mouse brain. A) Graphical representation of the 1mm amygdala punches. Image modified from Allen Brain Atlas. B) Top, Allen Brain Atlas *Tac2* mRNA levels expression by *in situ* hybridization (ISH), Bottom, ISH of *Tac2* mRNA levels performed in our lab. *Tac2* is expressed in: bed nucleus of the stria terminalis (white arrow), hypothalamus (green arrow), habenula (blue arrow), central amygdala (purple arrow), zona incerta (orange arrow) and medial mammillary nucleus (red arrow).

Home Cage vs 30 min after Fear Conditioning

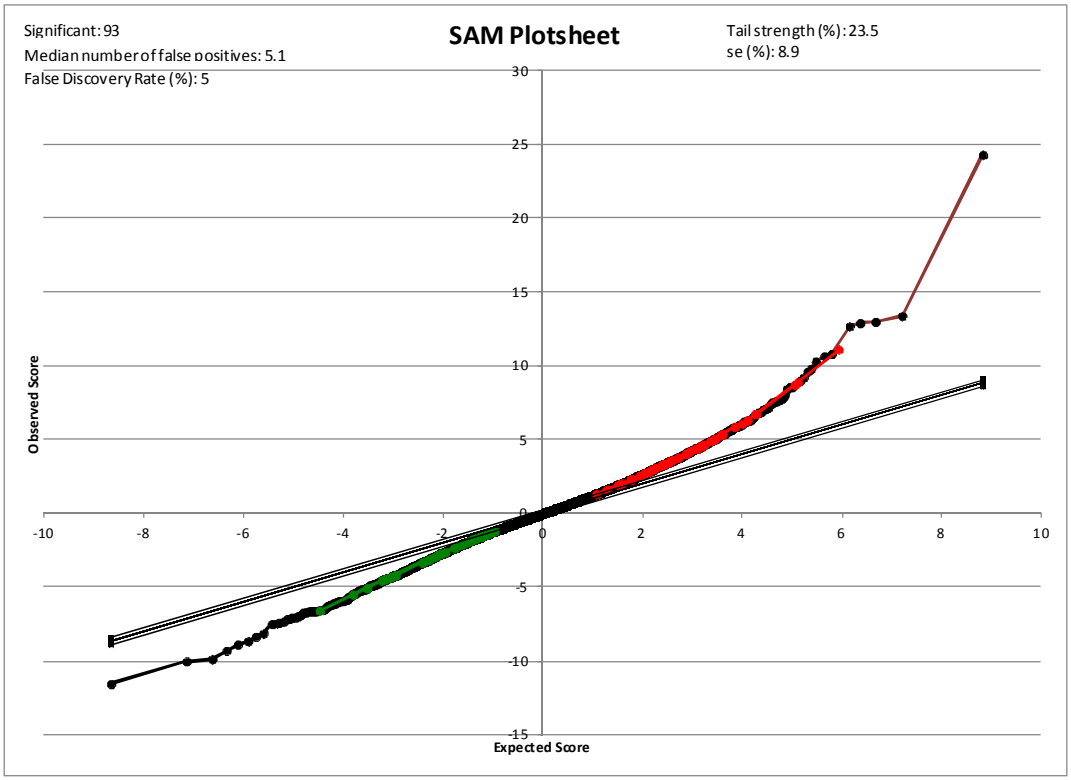

Home Cage vs 2hrs after Fear Conditioning

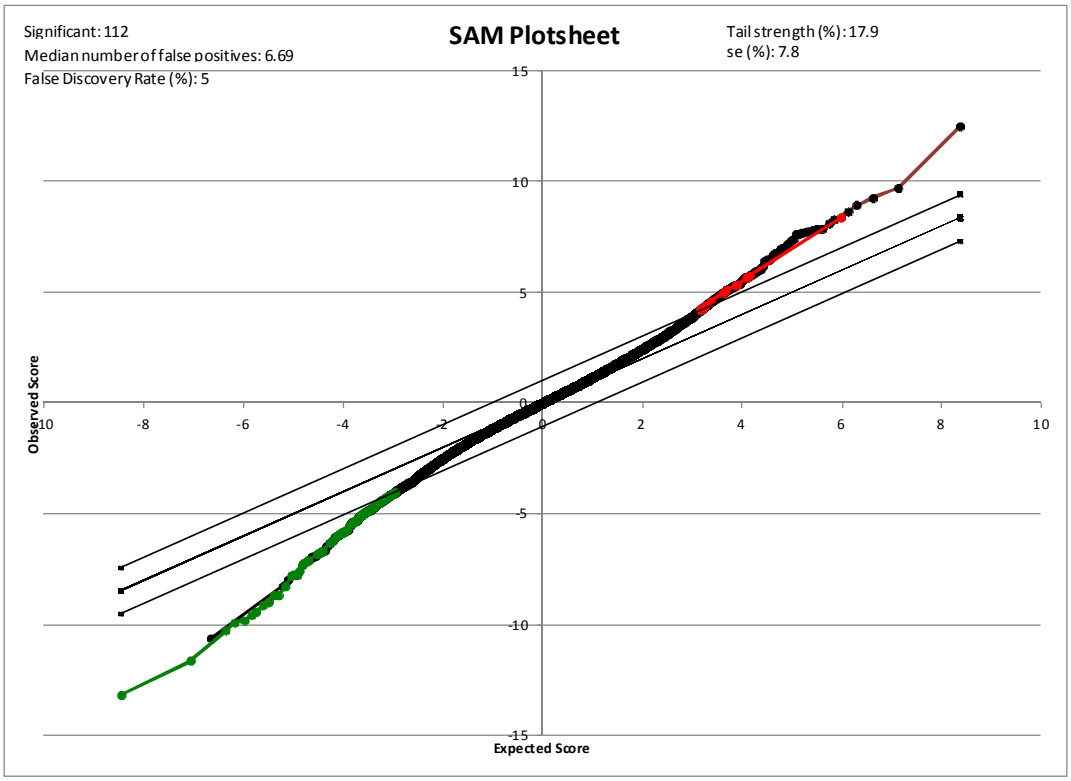

Figure S2, related to Figure 1. FDR analysis of the microarray.

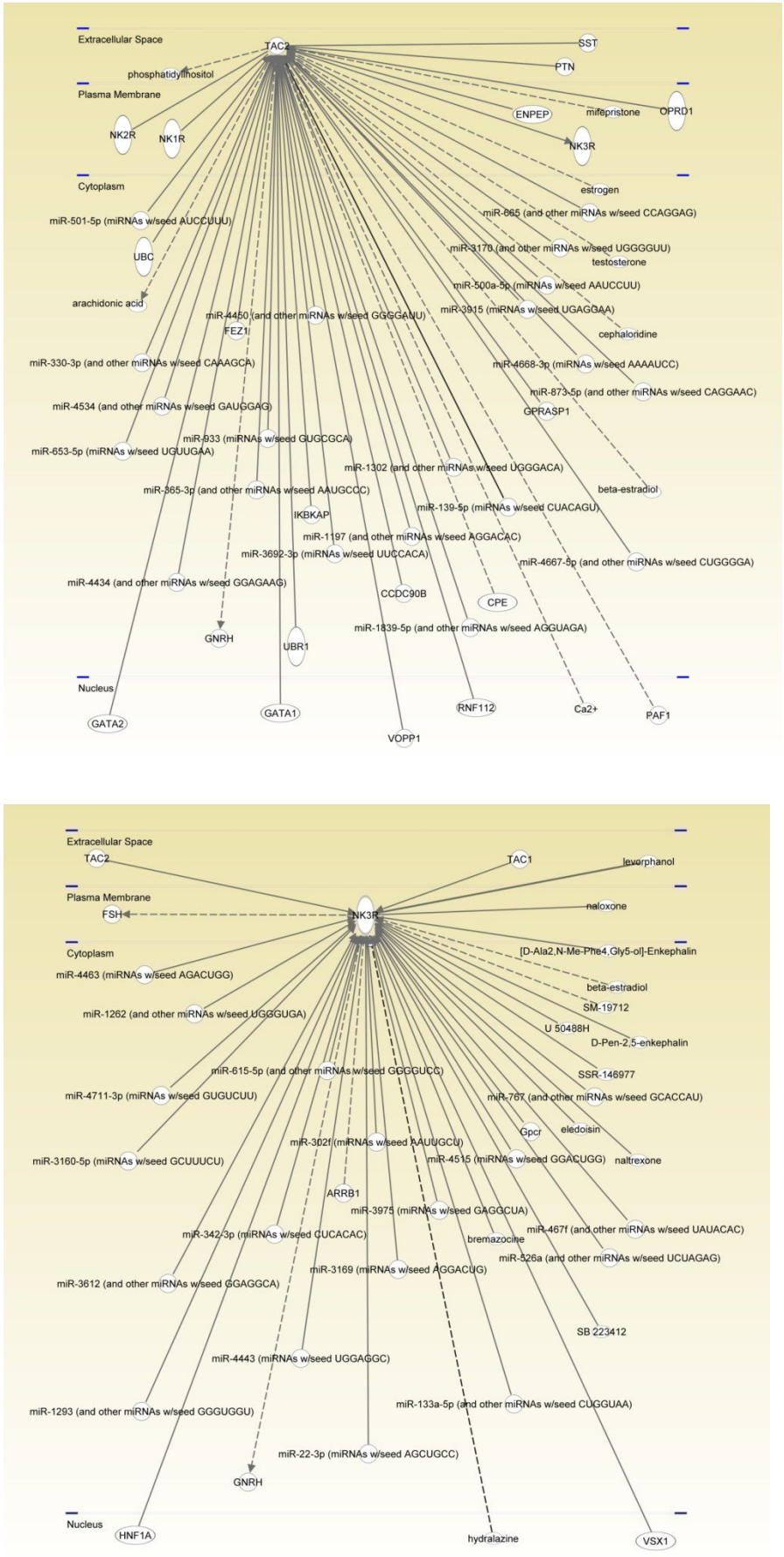

Figure S3, related to Figure 1. **Functional relationships of the *Tac2* gene and Nk3 receptor.** Previous published studies show the relationship of drugs, microRNAs, peptides and genes related to *Tac2* and Nk3R. Solid line: direct relationship. Dashed line: indirect relationship.

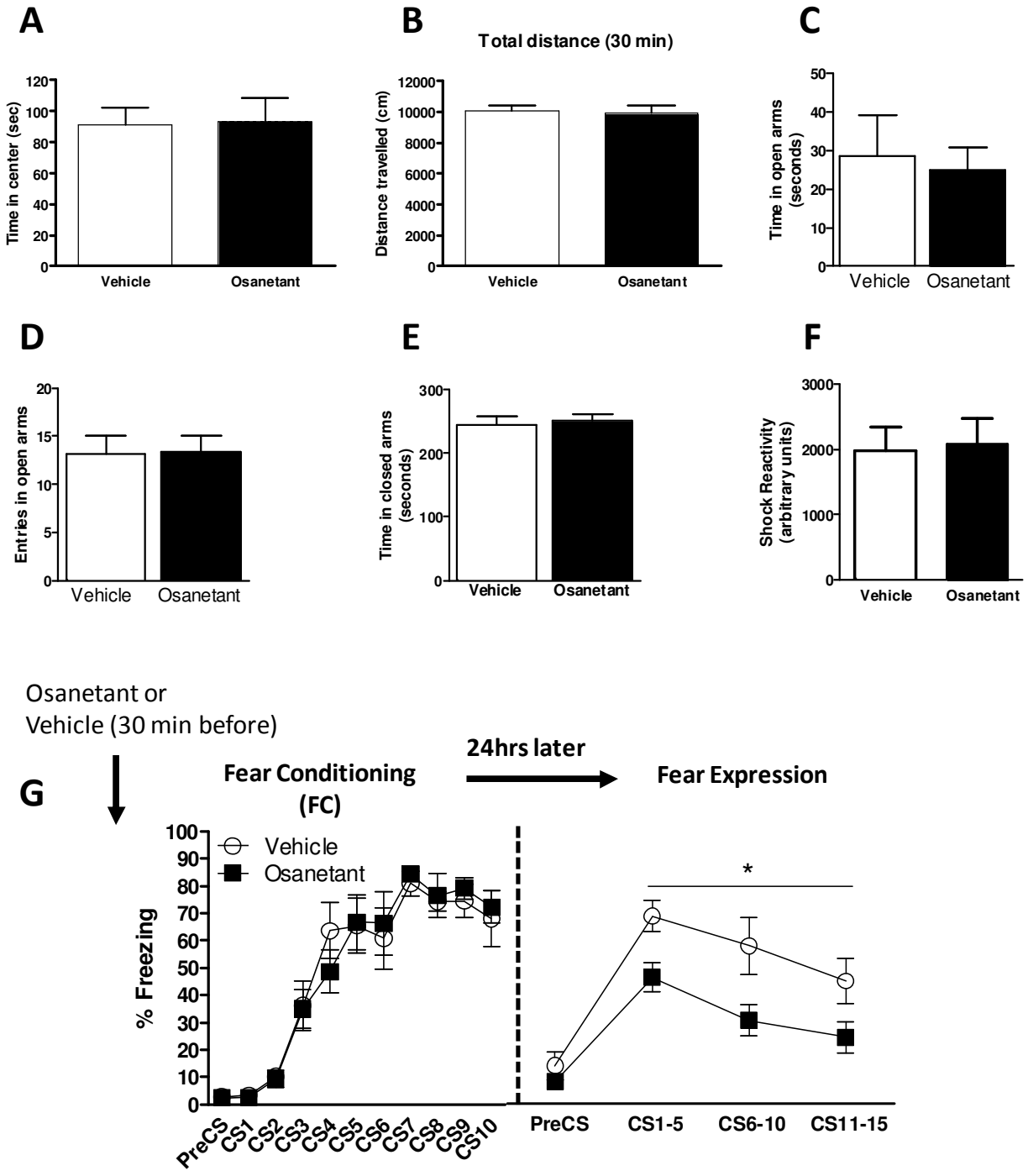

Figure S4, related to Figure 4. **Osanetant impairs fear learning with no effects on anxiety, locomotion nor shock reactivity.** Different cohorts of mice received systemic osanetant 30 minutes before open field, elevated plus maze or fear conditioning in the startle chamber. A) Osanetant did not modified anxiety-like behavior as shown by the time in the center of the open field. B) Animals receiving vehicle or osanetant showed equivalent distance travelled in the open field which indicates similar levels of locomotor activity. C, D and E) Osanetant did not modified anxiety-like behavior as shown by time in open arms, entries in open arms, and time in closed arms in the elevated plus maze. F) Equivalent shock reactivity shown when vehicle or osanetant was given 30 minutes before testing in the startle chamber. N=8 per group. G) Osanetant given systemically 30 minutes before FC impairs fear memory consolidation, without affecting fear expression, as shown by decreased freezing in the fear expression test. ANOVA repeated measures $F_{1,11} = 6.298$, *$P \leq 0.05$, N=6-7 per group. Mean ± SEM is shown.

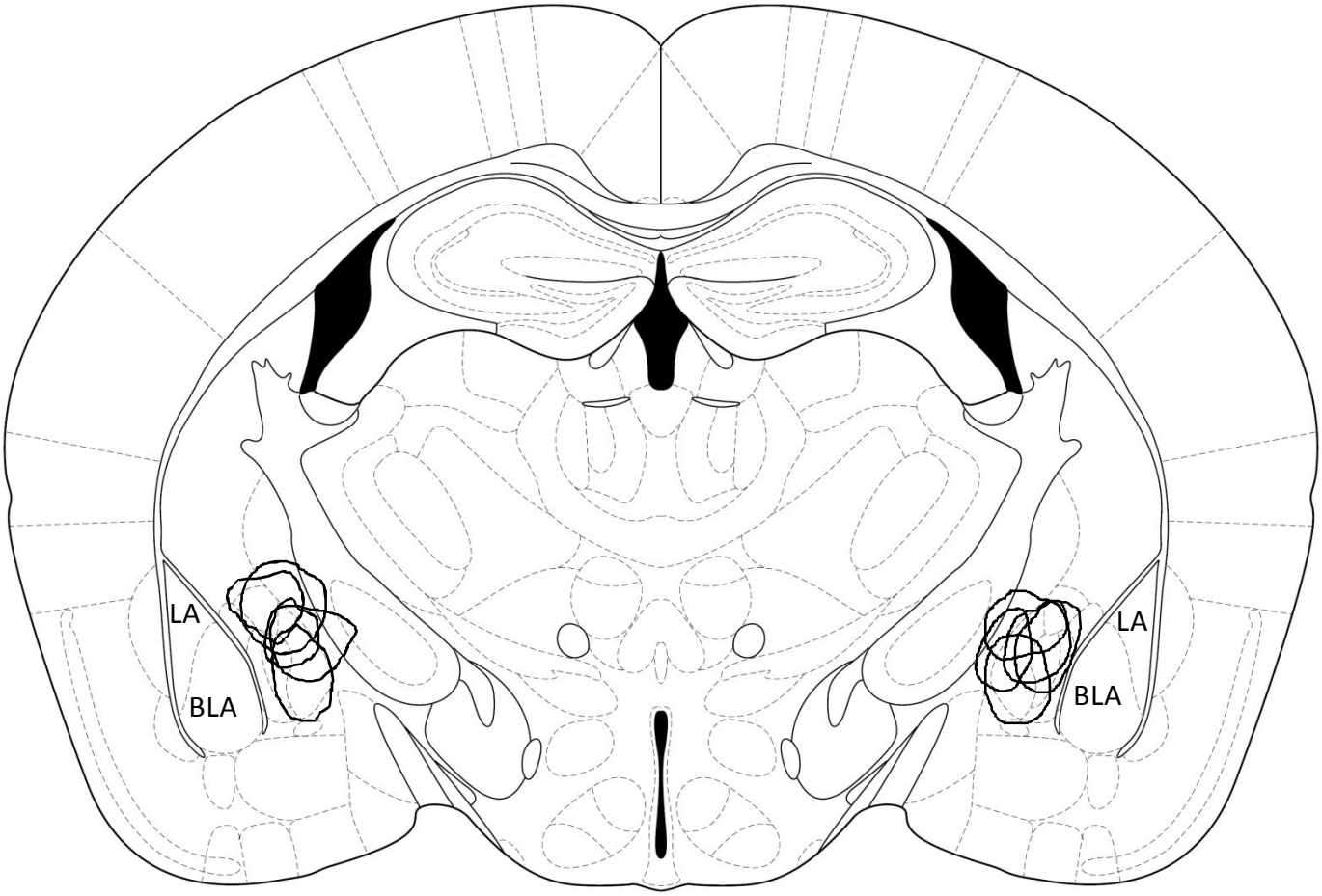

Figure S5, related to Figure 5. Graphical representation of the LV-*Tac2* overexpression in the CeA. Mice included in the analysis of the Lv-*Tac2* overexpression experiments had spread of infection in the CeA with no spread in BLA or LA.

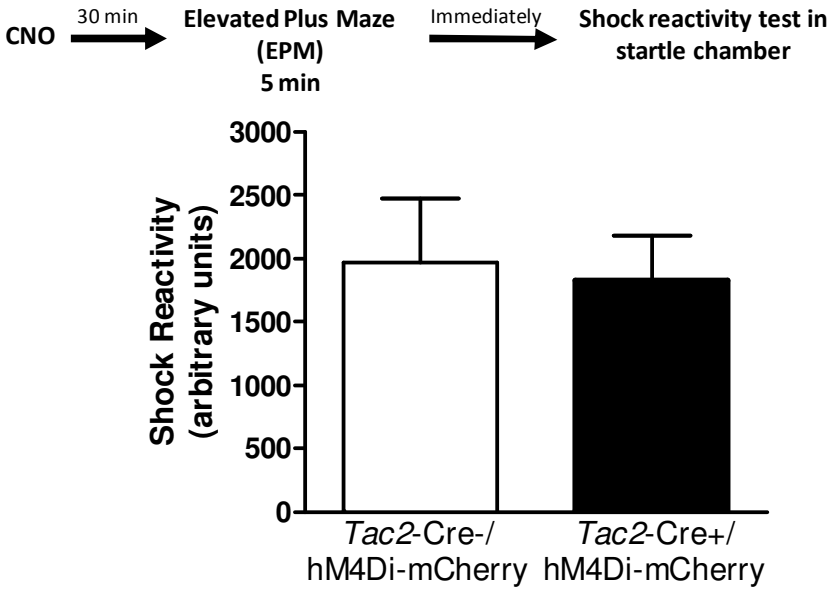

Figure S6, related to Figure 6. No differences in pain sensitivity when silencing the *Tac2*-expressing cells in the CeA. When CNO was given the two groups presented equivalent levels of shock reactivity suggesting no role in pain sensitivity of the *Tac2*-expressing cells in the CeA.

Home Cage vs 30 min after Fear Conditioning

Positive genes (47)							Specifically highly
Gene ID	Gene Name	Score(d)	Numerator(r)	Denominator(s+s0)	Fold Change	q-value(%)	expressed in Amygdala
ILMN_1215713	Egr4	11.09109	448.086375	40.40057155	2.020063897	0	No
ILMN_2623983	Egr2	8.853620456	181.111425	20.45619935	2.620265596	0	No
ILMN_2597827	Arc	8.685373586	227.156	26.15385484	2.062960434	0	No
ILMN_2993109	Ddit4	6.742796897	122.68755	18.19535007	1.605673321	0	Yes
ILMN_1240323	Dnajb1	6.740418626	667.968	99.0988894	1.514217387	0	No
ILMN_2621743	Gad1	6.267292315	900.255	143.6433718	1.582504861	0	No
ILMN_2428798	5031439G07Rik	6.067885974	193.230625	31.84480161	1.504898035	0	No
ILMN_2813484	Per1	5.823966409	186.076375	31.9501113	1.563814839	0	No
ILMN_2529458	LOC230253	5.345013621	368.137375	68.87491802	1.550070702	0	Not found
ILMN_2540574	LOC100039751	5.344190279	215.00095	40.23078123	1.554178757	0	Not found
ILMN_1249586	Hspa8	5.281728756	1035.7895	196.1080449	1.713159766	0	No
ILMN_2429164	Gnal	5.049234589	147.52105	29.21651735	1.528365177	0	No
ILMN_1229990	Agxt2l1	4.96592321	56.7663125	11.43117002	1.509492174	0	No
ILMN_2750515	Fos	4.874668724	251.5296	51.59932176	2.226992961	0	No
ILMN_2547305	Mobp	4.664755035	724.4794	155.3092059	1.763316284	0	No
ILMN_1213781	LOC100045668	4.64413152	690.0135	148.5775106	1.520478741	0	Not found
ILMN_3001914	Nfkbia	4.552292434	84.045925	18.46232996	1.584140663	0	No
ILMN_1214782	Pdcd4	4.525457379	73.20375	16.17598927	1.519919275	0	No
ILMN_2512204	mt-Nd4l	4.396633694	625.238475	142.2084528	1.564075602	0	Not found
ILMN_2666279	Arrdc3	4.343900064	136.096925	31.33058381	1.675007697	0	No
ILMN_1213954	Sgk1	4.189644324	2425.5965	578.9504579	2.153287601	0	Not found
ILMN_2778279	Fosb	4.031953893	109.0366625	27.04313229	2.001993665	0	No
ILMN_2589039	Cox6c	4.023569824	1099.80625	273.3409132	1.545000572	0	No
ILMN_2771036	Tac2	3.756458109	72.265125	19.23756978	1.530910817	0	Yes
ILMN_3150811	Tsc22d3	3.57891997	392.643425	109.7100322	1.704397662	0	No
ILMN_2629112	Asah3l	3.535665195	77.6940275	21.97437348	1.811136174	0	No
ILMN_2993334	Plekhf1	3.496372748	46.2280125	13.22170599	1.654636919	0	No
ILMN_2661820	Agxt2l1	3.431502545	57.9223425	16.87958605	1.648623678	0	No
ILMN_1259747	Il33	3.326436569	122.701225	36.88668713	1.620747847	0	No
ILMN_2690603	Spp1	3.297199418	113.0287725	34.28023549	1.825019843	0	No
ILMN_1236666	Acsl6	3.201617174	297.1804	92.82196586	1.549881389	0	No
ILMN_1248368	Mat2a	3.043517283	60.58362	19.90579135	1.541339255	0	No
ILMN_3097381	Mobp	2.98530051	254.12185	85.12437832	1.513612907	0	No
ILMN_1231336	Itih3	2.870127576	259.4255	90.38814239	1.549312667	0	No
ILMN_1243212	Sparc	2.806368689	105.97115	37.76095081	1.712435998	0	No
ILMN_2522571	Setd7	2.713503356	183.06635	67.46494327	1.529557587	0	No
ILMN_1251845	Slc10a4	2.680718709	91.694025	34.2050155	1.561757275	0	No
ILMN_3024681	Mobp	2.536998361	126.469225	49.84994352	1.644011426	1.44049643	No
ILMN_2829594	Hspa1a	2.306631118	44.44474	19.26824782	1.583647084	2.46345766	No
ILMN_2419660	mtDNA_ND4L	2.282619001	975.59975	427.4036751	1.687998977	2.46345766	Not found
ILMN_1221160	Unc13c	2.274301059	524.917	230.8036564	1.598185616	2.46345766	No
ILMN_1248947	Mal	2.244160184	412.900525	183.9888827	1.686683276	2.46345766	No
ILMN_2608073	Nap1l5	2.000841183	617.368925	308.554687	1.592422133	2.46345766	No
ILMN_2955509	Klk6	1.929954333	43.51373	22.54650758	1.564227411	2.46345766	No
ILMN_2851288	Ngfr	1.922101728	67.611325	35.17572666	1.520851164	2.46345766	No
ILMN_2971816	Gltp	1.908407039	212.9313	111.5754111	1.638608177	3.311271	No
ILMN_2776034	Gal	1.569722534	105.71999	67.34947591	1.918109421	4.66974116	Not found

Negative genes (46)							Specifically highly
Gene ID	Gene Name	Score(d)	Numerator(r)	Denominator(s+s0)	Fold Change	q-value(%)	expressed in Amygdala
ILMN_2445848	Zfp238	-6.604688573	-541.292825	81.95584379	0.633207945	0	No
ILMN_1231710	Crhbp	-5.507519811	-352.8114	64.05994207	0.617678069	0	No
ILMN_1237518	Dgkg	-5.076108892	-386.055525	76.05343644	0.647158987	0	No
ILMN_2512430	Zfp312	-4.568837049	-359.568	78.70011474	0.592832409	0	Not found
ILMN_2765047	Chrd	-4.477980048	-139.352375	31.11947206	0.611599623	0	No
ILMN_1225037	Grit	-4.429721111	-301.595725	68.08458534	0.651824595	0	No
ILMN_1233537	Gucy1a3	-4.343009636	-177.507325	40.87196204	0.60642504	0	No
ILMN_2631143	Sox5	-4.327509869	-224.538875	51.88639236	0.622381127	0	No
ILMN_2754435	Ldb2	-4.206027498	-299.18965	71.13354588	0.657705278	0	No
ILMN_1237666	Hgf	-4.193621664	-51.934115	12.38407257	0.663565557	0	No
ILMN_1239134	Lypd1	-3.349608084	-1916.94025	572.287922	0.613051267	0	No
ILMN_2699052	Nrn1	-3.31875933	-744.9555	224.4680695	0.641760953	0	No
ILMN_2658266	Gpr22	-3.214432735	-128.865375	40.08961631	0.638597412	0	No
ILMN_1218051	Iqgap2	-3.111689509	-69.876375	22.4560885	0.649643389	0	No
ILMN_2610744	Myl4	-2.943877654	-276.3328	93.86694436	0.654627582	0	No
ILMN_1221503	Ccnd1	-2.837528141	-229.524675	80.88895109	0.658258852	0	No
ILMN_2521965	Slc30a3	-2.761973893	-558.334725	202.1506164	0.60354295	0	No
ILMN_2708203	Cdkn1c	-2.746141043	-266.22635	96.94562146	0.584778394	0	No
ILMN_1253365	Lypd1	-2.626335409	-54.6324925	20.80179565	0.638234585	0	No
ILMN_2441534	Rsph1	-2.358040688	-175.1799	74.29044839	0.614479793	1.44049643	No
ILMN_1235124	Thsd4	-2.310002725	-82.00105	35.49824817	0.616168822	1.44049643	No
ILMN_2965903	Hdc	-2.126254237	-82.24245	38.67949965	0.641656418	2.61505505	No
ILMN_2462222	Trpm3	-2.001557192	-93.0324	46.48001084	0.480451755	2.61505505	No
ILMN_3098069	Trpm3	-1.859884751	-79.73005	42.86827449	0.538840229	2.61505505	No
ILMN_1239718	Tekt1	-1.811694221	-56.7152425	31.3050855	0.63055611	2.61505505	No
ILMN_2425028	LOC675572	-1.801794131	-68.9699775	38.27850048	0.586268448	2.61505505	Not found
ILMN_1223317	Lgals3	-1.740191903	-58.15569	33.41912458	0.659788291	2.61505505	No
ILMN_1236788	Igfbp2	-1.73087102	-75.2429525	43.47114929	0.589684943	3.311271	No
ILMN_1231588	1110059M19Rik	-1.722270889	-41.34386	24.00543391	0.652319573	3.311271	Not found
ILMN_2599861	Defb11	-1.614213477	-95.2135875	58.98450785	0.562523485	3.311271	No
ILMN_1231445	Inmt	-1.614170179	-69.865225	43.28244068	0.659273264	3.311271	No
ILMN_3000679	Folr1	-1.594562306	-103.1028275	64.65901463	0.565961557	3.311271	No
ILMN_2625855	Gpx8	-1.583467848	-125.847775	79.47605323	0.638051159	3.311271	No
ILMN_2827072	Slc13a4	-1.539087861	-224.576725	145.9154676	0.534402508	3.311271	No
ILMN_2980323	Cldn2	-1.535196244	-89.83698	58.51823853	0.624617041	3.311271	No
ILMN_1236758	Wfdc2	-1.531491326	-160.099015	104.5379835	0.532467445	3.311271	No
ILMN_1246173	Msx1	-1.474867165	-117.485325	79.65824162	0.592201378	3.311271	No
ILMN_1255479	Cldn2	-1.469922793	-84.461285	57.45967435	0.597583436	3.311271	No
ILMN_2667635	Clic6	-1.435307199	-459.048725	319.8261149	0.639071004	3.311271	No
ILMN_2756486	Aqp1	-1.431527143	-143.53467	100.2668169	0.597075016	3.311271	No
ILMN_1215019	Dynlrb2	-1.387852728	-99.935385	72.00719715	0.624702255	4.66974116	No
ILMN_1221292	Rdh5	-1.384413084	-135.0119	97.52284311	0.62760043	4.66974116	No
ILMN_1249135	D230046H12Rik	-1.35015035	-170.0683	125.9624901	0.631374711	4.66974116	Not found
ILMN_2617005	Prlr	-1.311424762	-249.72025	190.4190445	0.584598746	4.66974116	No
ILMN_2714278	2810046M22Rik	-1.281005496	-58.9134125	45.98997636	0.653221478	4.66974116	Not found
ILMN_1253148	Kl	-1.267334037	-154.62475	122.0078886	0.649612582	4.66974116	No

Table S1, related to Figure 1. Genes regulated 30 minutes after auditory fear conditioning in the amygdala.

Home Cage vs 2hrs after Fear Conditioning

Positive genes (12)							Specifically highly expressed in Amygdala
Gene ID	Gene Name	Score(d)	Numerator(r)	Denominator(s+s0)	Fold Change	q-value(%)	
ILMN_1231471	Zfp94	8.386723674	66.2835	7.903384275	1.301567758	0	No
ILMN_1237651	Ipp	5.746539969	56.152	9.77144513	1.37053424	2.02653732	No
ILMN_1254047	Slc26a9	5.668839016	17.0027025	2.999327102	1.34624468	2.02653732	No
ILMN_1243082	6330500D04Rik	5.354314626	90.828175	16.96354834	1.411632418	2.70204976	No
ILMN_3082287	4933421E11Rik	5.324176547	93.616375	17.58325896	1.328562119	2.70204976	No
ILMN_2778438	A830006F12Rik	5.097568509	69.35875	13.60624185	1.350980686	2.70204976	No
ILMN_2635348	Iqcb1	4.985462711	128.6372	25.80245956	1.313235676	3.61490441	No
ILMN_1235689	Wdr37	4.575952594	79.6495	17.40610253	1.38320816	4.36146075	No
ILMN_1228782	Lphn1	4.407098228	179.181	40.65736472	1.385366852	4.50341627	No
ILMN_1225818	Tia1	4.355954051	62.014975	14.23682947	1.383160487	4.90831057	No
ILMN_2602140	Eif2b5	4.298254351	144.87875	33.70641618	1.307686876	4.90831057	No
ILMN_3150996	Blm	4.288696809	35.1514275	8.196295767	1.347426464	4.90831057	No

Negative genes (100)							Specifically highly expressed in Amygdala
Gene ID	Gene Name	Score(d)	Numerator(r)	Denominator(s+s0)	Fold Change	q-value(%)	
ILMN_2742647	EG666609	-13.18903005	-360.23875	27.31351347	0.765483534	0	Not found
ILMN_2534572	LOC272681	-11.63439244	-1281.894	110.1814304	0.710609467	0	Not found
ILMN_1232890	Rpl32	-10.26487319	-759.56925	73.99694432	0.688632154	0	No
ILMN_2542885	Wdr89	-9.914390811	-29.2099775	2.946220101	0.6924394	0	No
ILMN_1245034	LOC382061	-9.807881635	-64.69765	6.596495799	0.747901604	0	No
ILMN_1242465	LOC231368	-9.562144643	-332.1655	34.73755234	0.606910107	0	No
ILMN_1244853	LOC100044948	-9.424660492	-228.61865	24.2574945	0.72541822	0	No
ILMN_1253958	EG237361	-9.116487212	-68.27585	7.489271735	0.713652393	0	No
ILMN_1251729	Nfe2l1	-8.986447765	-576.07125	64.10444539	0.721485902	0	No
ILMN_1227006	Scnm1	-8.677677434	-74.744825	8.613459715	0.714107678	0	No
ILMN_2467534	Ide	-8.664299555	-33.1442475	3.82538107	0.68713343	0	No
ILMN_1249586	Hspa8	-8.261388059	-647.059	78.32327877	0.691796497	0	No
ILMN_1242107	Cox7a2l	-7.820227063	-363.47725	46.47911717	0.765777047	0	No
ILMN_1232274	LOC100048508	-7.762831146	-172.258375	22.19014838	0.65375335	0	No
ILMN_1250136	LOC433943	-7.733649127	-113.805875	14.71567602	0.686031214	0	No
ILMN_2801790	Chmp2a	-7.586073989	-215.54315	28.41300392	0.713615993	0	No
ILMN_1239293	Sulf2	-7.31719927	-101.3827	13.85539689	0.644239178	0	No
ILMN_2691261	Ndufb10	-7.231030885	-199.951125	27.65181455	0.651046482	0	No
ILMN_2753649	Arpc1a	-7.206729408	-470.38175	65.26979485	0.7327373	0	No
ILMN_1218976	EG432681	-7.104605265	-1063.466	149.6868525	0.72935339	0	Not found
ILMN_1213781	LOC100045668	-7.098802987	-906.92625	127.7576306	0.593790195	0	Not found
ILMN_2771991	Ndrg2	-6.815501166	-343.0758	50.33757484	0.671707012	0	No
ILMN_1243433	LOC100048037	-6.767702045	-327.85595	48.4442057	0.681415218	0	Not found
ILMN_1239211	LOC100047935	-6.761295386	-1030.80025	152.4560297	0.585223928	0	Not found
ILMN_2998173	EG625054	-6.722215024	-1568.40225	233.316287	0.715198481	0	Not found
ILMN_2482571	Flnb	-6.6674168	-40.0092	6.0007048	0.763066856	0	No
ILMN_2527129	LOC329750	-6.298088057	-107.111675	17.00701451	0.753203711	0	Not found
ILMN_2768972	Fam107a	-6.269969641	-509.48225	81.25753061	0.704283425	0	No
ILMN_1229517	Ftl1	-6.209956846	-203.890975	32.83291334	0.763164682	0	Not found
ILMN_2985282	Peci	-6.024585368	-55.4373	9.201844877	0.752201725	0	No
ILMN_2716098	Hsp105	-5.953547861	-486.331	81.68759391	0.700583081	0	No
ILMN_2522542	Klhdc5	-5.892894671	-24.86875	4.22012464	0.762565075	0	No
ILMN_1240350	LOC380692	-5.865046433	-590.50225	100.6815985	0.711629081	0	Not found
ILMN_1243988	LOC269251	-5.837333461	-45.769075	7.840750457	0.749725599	0	Not found
ILMN_1241383	Scrn1	-5.831562089	-118.1703	20.26391869	0.765772611	0	No
ILMN_1227972	Rps16	-5.825457519	-677.93525	116.3745934	0.731400267	0	No
ILMN_1213364	LOC638892	-5.815671661	-70.044275	12.04405597	0.729741208	0	Not found
ILMN_1230065	LOC245892	-5.785888806	-56.2077	9.714618079	0.713384463	0	Not found
ILMN_1249235	LOC668387	-5.774767235	-150.013975	25.97749293	0.672015451	0	Not found
ILMN_1225930	LOC100039346	-5.74024713	-173.251625	30.18191048	0.711070973	0	Not found
ILMN_2932359	Tpi1	-5.561411051	-497.852925	89.51917426	0.663470887	0	No
ILMN_1230620	LOC100039786	-5.422858106	-294.462	54.30014842	0.684022796	0	Not found
ILMN_2723474	Adcy9	-5.353195399	-37.860525	7.072509441	0.75213138	1.68240834	No
ILMN_2486012	C330006P03Rik	-5.352651074	-297.18535	55.52115127	0.709438103	1.68240834	No
ILMN_1214918	LOC546015	-5.350362671	-232.924125	43.53426848	0.73767308	1.68240834	No
ILMN_1260088	LOC100043527	-5.348052949	-808.25525	151.1307494	0.627012194	1.68240834	No
ILMN_2482572	Flnb	-5.345779391	-44.750325	8.37115072	0.728672075	1.68240834	No
ILMN_2499944	Tomm7	-5.343228766	-278.244225	52.0741741	0.765538179	1.68240834	No
ILMN_2534329	LOC333841	-5.295236894	-15.536425	2.934037761	0.759806413	1.68240834	Not found
ILMN_2946901	Slc25a38	-5.27129372	-20.4219775	3.874186981	0.763533139	1.68240834	No
ILMN_1246148	Dgkd	-5.251507215	-182.550975	34.76163462	0.746338965	1.68240834	No
ILMN_2668083	LOC668706	-5.107626296	-453.829	88.8532116	0.75166404	3.07474628	Not found
ILMN_1222723	LOC668239	-5.094324315	-567.32775	111.3646707	0.734652623	3.07474628	Not found
ILMN_1243991	LOC433476	-5.065888025	-45.5451	8.990546135	0.768794452	3.07474628	Not found
ILMN_1233252	Rnu65	-5.059200088	-49.325975	9.749757697	0.73718023	3.07474628	Not found
ILMN_3129825	Prosc	-4.998414849	-54.278275	10.85909766	0.739032075	3.07474628	No
ILMN_2871262	Bcap31	-4.991386447	-105.9871	21.23400004	0.743182016	3.07474628	No
ILMN_1258613	N4wbp5-pending	-4.975576415	-427.217	85.86281555	0.7243551	3.07474628	Not found
ILMN_1220739	Nsg2	-4.975203983	-636.5485	127.9442013	0.668995094	3.07474628	No
ILMN_2987984	S100a13	-4.970119796	-43.36135	8.724407414	0.738764859	3.07474628	No
ILMN_1216674	LOC234882	-4.891947016	-163.12305	33.3452201	0.737577821	3.07474628	Not found
ILMN_2752234	Krba1	-4.888695317	-94.973625	19.4271925	0.670692814	3.07474628	No
ILMN_2958159	Eno1	-4.874704701	-522.02175	107.0878714	0.761496874	3.07474628	No
ILMN_2712731	Phf10	-4.855598507	-31.12528	6.410184029	0.751426152	3.61490441	No
ILMN_1216732	Mcl1	-4.854270081	-129.07245	26.58946615	0.764941821	3.61490441	No
ILMN_1235982	Rai12	-4.81287285	-195.181925	40.55414118	0.736804591	3.61490441	No
ILMN_2809247	Tmem85	-4.772755929	-480.29525	100.6326863	0.697876639	3.61490441	No
ILMN_3052685	Tro	-4.720099446	-133.132975	28.20554451	0.643621907	3.61490441	No
ILMN_1246446	Lrrc59	-4.693738614	-35.001425	7.457046052	0.766170294	3.61490441	No
ILMN_1232692	LOC383712	-4.673599178	-720.3005	154.1211543	0.728664377	3.61490441	Not found
ILMN_3028324	Tug1	-4.654063073	-44.47575	9.556327299	0.736455539	3.61490441	No
ILMN_2533188	LOC270037	-4.600512794	-282.375175	61.37906525	0.766155508	3.61490441	Not found
ILMN_1239742	Atp2a2	-4.58917178	-614.0235	133.7983256	0.746573246	3.61490441	No
ILMN_1234256	LOC668038	-4.581855022	-69.16475	15.09535978	0.607381415	3.61490441	Not found
ILMN_2529458	LOC230253	-4.574068601	-387.989875	84.82379886	0.633017844	3.61490441	Not found
ILMN_2636666	Prodh	-4.573625906	-64.474525	14.09702637	0.74360861	3.61490441	No
ILMN_2745555	Mrps21	-4.547654477	-120.17575	26.42587527	0.756152953	3.61490441	No
ILMN_2673936	Rpl18a	-4.538887657	-385.112575	84.84734677	0.60932979	3.61490441	No
ILMN_2685275	Tmem109	-4.52986409	-192.718975	42.5440965	0.741361579	3.61490441	No
ILMN_2961626	Them2	-4.502373129	-304.5518	67.64250569	0.753046168	4.36146075	No
ILMN_1254705	Atp5d	-4.488316398	-289.8215	64.5724308	0.763689674	4.36146075	No
ILMN_1228717	LOC225134	-4.471862718	-317.0271	70.89374607	0.704810537	4.36146075	Not found
ILMN_2654896	LOC100047998	-4.456102818	-940.95175	211.1602421	0.709409784	4.36146075	Not found
ILMN_2649671	Ipas	-4.444285179	-45.4406875	10.22452108	0.609141953	4.36146075	No
ILMN_2778279	Fosb	-4.408031465	-39.9288625	9.058207234	0.731568101	4.36146075	No
ILMN_2856986	Scg3	-4.376487727	-297.1398	67.89458089	0.739407857	4.36146075	No
ILMN_2595967	LOC100039532	-4.364042425	-725.55525	166.2576069	0.721592405	4.50341627	Not found
ILMN_1227653	Rpl27a	-4.351754551	-520.93175	119.7061424	0.756792438	4.50341627	No
ILMN_2776419	Dnclc1	-4.316124241	-158.008525	36.60889172	0.748753305	4.50341627	No
ILMN_2873112	Mdh2	-4.286646495	-158.318725	36.93300234	0.65157353	4.50341627	No
ILMN_2665229	LOC100041864	-4.214222722	-834.0045	197.902331	0.724290952	4.50341627	Not found
ILMN_1244913	Ryr2	-4.211551219	-175.326875	41.62999946	0.717144061	4.50341627	No
ILMN_2710185	Mylc2b	-4.207075125	-194.656175	46.26876612	0.621083914	4.50341627	No
ILMN_2522145	C77604	-4.204517158	-60.882525	14.48026556	0.757472895	4.50341627	No
ILMN_3004441	Atp5h	-4.192382168	-432.5921	103.1852733	0.671487046	4.90831057	No
ILMN_1238389	2310022M17Rik	-4.155535283	-51.79595	12.46432685	0.711703084	4.90831057	Not found
ILMN_2637233	Prdx5	-4.155530857	-81.9445	19.71938191	0.755557871	4.90831057	No
ILMN_1246650	Hsp90ab1	-4.113986753	-336.77655	81.86135986	0.673862227	4.90831057	No
ILMN_1254302	Nsfl1c	-4.098591145	-132.7612	32.3919111	0.731340721	4.90831057	No
ILMN_2651886	Pgk1	-4.057600785	-464.05625	114.367153	0.703175541	4.90831057	No

Table S2, related to Figure 1. Genes regulated 2 hours after auditory fear conditioning in the amygdala.

Supplemental Experimental Procedures

Mice

Amygdala cell culture experiments were performed with male wild-type (WT) C57BL/6J p21 mice. All other experiments were performed on adult WT strain C57BL/6J or B6.129-*Tac2*tm1.1(cre)Qima/J (*Tac2*-Cre) (Mar et al., 2012) from Jackson Labs (Stock # 018938), male mice that were group-housed in a temperature-controlled vivarium, with *ad libitum* access to food and water. Animals were maintained on a 12-hour/12-hour light/dark cycle, with all behavioral procedures being performed during the light cycle. All procedures used were approved by the Institutional Animal Care and Use Committee of Emory University and in compliance with National Institutes of Health (NIH) Guide for the Care and Use of Laboratory Animals.

Immobilization to wooden board (IMO)

Immobilization procedures were conducted in a room separate from behavioral testing apparatus. Each animal was immobilized by gently restraining its four limbs in a prone position to metal arms attached to a wooden board for 2 hours. All animals of the same cage received the same treatment—either immobilization or handling. After treatment, animals were returned to their home cage and remained undisturbed until fear training (Andero et al., 2011 and Andero et al., 2013).

mRNA extraction and microarray

Mice were sacrificed and brains were immediately fresh frozen on dry ice and stored at -80ºC. Amygdala tissue from both hemispheres was extracted by 1mm micropunch and each structure from each mouse was individually stored. Total RNA was isolated and purified from the tissue with the RNeasy Mini Kit catalog # 74106 (Qiagen) following the manufacturer's instructions. We obtained ~2 ug RNA per side

for a total of ~4 ug per brain. Amygdala tissue was used with 4 animals per condition. Electrophoresis assay and electropherogram to ensure the RNA quality was performed with Agilent 2100 BioAnalyzer PicoChip (Agilent Technologies) before the microarray. Illumina Mouse WG-6 v2 Expression BeadChip microarray (Illumina, Inc.) was assayed for 45,281 transcripts. RNA quality control, hybridizations and preliminary data analysis were conducted at the Cancer Genomics shared resource, Winship Cancer Institute (Emory University). The heat map was created with Genesis 1.4.0 (Sturn et al., 2002). FDR was calculated with SAM 4.01 using a standard 5% cutoff criteria. The cutoff criteria was set with an FDR at the 1.3 fold level for the 2hrs after fear conditioning (FC) group, since with the more conservative 1.5 fold cutoff used in the 30 min after FC group , no genes were initially identified. The criteria followed in Supplemental Table 1 and 2 for a Yes in the column "Specifically highly expressed in the amygdala": 1) Very high expression in the amygdala (red color) 2) No expression of the gene in the hippocampus nor PFC (other key areas related to emotional learning). The search was performed on March 2014 in the Allen Brain Atlas. The pathway analysis was generated through the use of IPA (Ingenuity® Systems, www.ingenuity.com)

Complementary DNA synthesis and qPCR

RNA isolation for q-PCR was performed as described above in a different cohort of animals than the microarray. Total RNA was reverse transcribed using the RT2 First Strand Kit catalog # 330401 (Qiagen) according to the manufacturer's instructions. The primers used for the qPCR were TaqMan Tac2 Mm01160362_m1, ADCYAP1R1 Mm01326453_m1 and NK3R Mm00445346_m1 from Applied Biosystems. q-PCR thermal cycling parameters were 10 minutes at 95°C, followed by 40 cycles of amplifications for 15 seconds at 95°C, 1 minute at 60°C. A dissociation stage, consisting of 15 seconds at 95°C, 1 minute at 60°C, and 15 seconds at 95°C, was added at the end. Quantification of mRNA was performed using the Applied Biosystems 7500 Real-Time PCR System. Relative levels of mRNA expression were normalized in all the samples with expression levels of glyceraldehyde- 3-phosphate dehydrogenase (GAPDH). Graphics are represented by fold change obtained with the 2^-ddCt method (Andero et al., 2013).

Elevated plus maze

The elevated plus maze consisted of two open arms (50 × 6.5 cm) and two closed arms with a wall (50 × 6,5 × 15 cm) attached to a common central platform (6,5 × 6,5 cm) to form a cross. The maze was elevated 65 cm above the floor. Test sessions lasted 5 minutes and behaviors were continuously recorded using a video camera placed over the apparatus. Activity was analyzed with stopwatch by a researcher blind to the each mouse treatment. Arm entry was considered complete if all four paws entered a closed or open arm from the central platform (Andero et al., 2013)

Open Field

The open field was an open box (27,9cm x 27,9cm) made of Plexiglas. The mice were placed in the apparatus to explore for 30 min, and then returned to home cages. Locomotor and center/periphery activity data was obtained by a video camera placed over the apparatus and analyzed using the SMART 2.5.19 video-tracking system (Panlab, Harvard Apparatus) (Andero et al., 2013).

Cued-Fear Conditioning and Fear Expression test

Mice were given fear conditioning and fear expression in standard rodent modular test chambers (ENV-008-VP; Med Associates Inc) with an inside area of 30,5cm (L) x 24,1cm (W) x 21,0cm (H). Mice were given a 10-minutes chamber exposure session to habituate mice to handling and the training context. Mice that had immobilization stress were habituated to the test chambers before the stress session. The two habituation days were carried out the same days for all mice, independently if they were going to be submitted to the stress procedure or not. The tone conditioned stimulus was generated by a Tektronix function generator audio oscillator delivered through a high-frequency speaker (Motorola, Model 948) attached to side of each chamber. Mice received 5 or 10 trials of a conditioned stimulus (CS) tone (30 seconds, 6 kHz, 70 db) co-terminating with a US footshock, 500ms, 1mA. Retraining of mice (Figure 6E) was performed with a 12 kHz tone. The expression of fear was assessed 24 hours after fear conditioning and

consisted of 15 CS tone trials (30 s each) with a 1.5 minutes inter-trial interval (ITI). Tone presentation and freezing data were controlled, stored, and analyzed with FreezeView software (Coulbourn Instruments) (Andero et al., 2011, Andero et al., 2013).

Shock reactivity

Shock reactivity was assessed in startle-footshock chambers (SRLAB, San Diego Instruments) consisting of a nonrestrictive acrylic plastic cylinder, 5,5 cm in diameter and 13 cm long, mounted on a Plexiglas platform which was located in a ventilated, sound-attenuated chamber. The footshock, US, was delivered through a removable stainless steel grid floor using one of four constant current shock generators (SDI, San Diego, CA) located outside the isolation chambers. A piezoelectric accelerometer mounted under each platform detected cylinder movements that were digitized and stored by an interfacing computer assembly. Shock reactivity was defined as the peak activity/accelerometer voltage that occurred during the 200 ms after the onset of the US. Response sensitivities were calibrated (SR-LAB Startle Calibration System) to be nearly identical in all startle cylinders. The tone CS was generated by a Tektronix function generator audio oscillator (Model CFG253, Beaverton, OR) and delivered through a high-frequency speaker (Motorola, Model 948) located 13 cm from the rear of each sound intensities were measured by an audiometer (Radio Shack, Ft. Worth, TX, #33-2055). Stimuli presentation and data acquisition were controlled, digitized and stored by an interfacing IBM PC compatible computer using SRLAB software. On each of 2 days prior to training, mice were given a 10- minutes startle chamber exposure session to habituate mice to handling and the training context. During cued fear training used to measure shock reactivity, mice received 5 trials of a conditioned stimulus tone (30 s, 6 kHz, 70 db) co-terminating with a US footshock 500ms, 1mA. The inter-trial training interval was 5-min (Andero et al., 2011).

Radioactive in situ hybridization

The full-length clone used was obtained as expressed sequence tag clones from the NIH IMAGE database (ATCC, Manassas, VA): *Tac2* in pT7T3D (GI: 1533442). *In situ* hybridization was performed with antisense riboprobes after sequence verification of the clones. All clones analyzed were 90% homologous with mouse coding sequence as determined by National Center for Biotechnology Information basic local alignment search tool. *In situ* hybridization was performed as follows. Mice were killed by chloral hydrate overdose. Brains were rapidly removed and frozen in dry ice and stored at -80°C. Brains were sectioned at 16 μm thickness on a Leica Cryostat (Nussloch, Germany) at -20°C onto gelatin-coated slides. Sections were placed on 20 consecutive slides per brain, such that each slide contained similar sections of brain. Following a prehybridization procedure, the sections were hybridized as described previously (Rattiner et al., 2004b). [35S]UTP (1250 Ci/mmol, 12.5 mCi/ml; DuPont NEN, Boston, MA)-labeled riboprobes were prepared from linearized clones using T7 polymerase at high specific activity by only using radioactive UTP in the polymerase reaction, with around 20% incorporation. After preparation of full-length antisense RNA strands, the RNA was base hydrolyzed to average lengths of 50–100 bp and isolated using a Sephadex gravity flow column. Hybridizations were performed under Parafilm at 52°C overnight. Slides were then stringently washed, dried, and placed against Kodak (Rochester, NY) magnetic resonance autoradiography film for 5-30 days. Films were scanned into a desktop computer at 600 dpi, and images were analyzed with Adobe Systems (San Jose, CA) Photoshop software. Hybridization density quantification was performed with the mean luminosity histogram feature of Adobe Photoshop. This measure was shown to produce linear densities with 14C radiation standards with the exposure times and levels used. Within one experiment, all slides hybridized to the same probe were exposed to the same piece of film. This ensured equivalent exposure times and conditions between animals and experimental groups. For each section, hybridization density was determined for the regions of interest (ROI), as well as an adjacent background area that lacks hybridization (e.g., hippocampus). For each section normalized density (ROI density - background density). The normalized densities from two different cryostat sections per brain were examined and averaged to give the density for each individual per ROI. For each experimental group, hybridization density is reported as the average density of all individual animals for that condition (Rattiner et al., 2004b). Mice included in the

analysis of the Lv-*Tac2* overexpression experiments had spread of infection in the CeA with no spread in BLA or LA.

Fluorescent in situ hybridization (FISH)

Mice were anesthetized and decapitated. Brains were rapidly removed, frozen on dry ice, and stored at -80°C until processing. Tissue was sectioned at 16 μm on a cryostat and mounted on Superfrost Plus slides (Fisher Scientific). The full-length clones used were obtained as expressed sequence tag clones from the NIH IMAGE database (ATCC, Manassas, VA): *Tac2* in pT7T3D (GI: 1533442), *PKCd* in pCMV-SPORT6 (GI: 6515302), *Enk* in pDNR-LIB (GI: 6774387). cRNA riboprobes were prepared from linearized constructs for antisense sequences of *Tac2*, *PKCd* and *Enkephalin* (T7 RNA polymerase) as previously described (Jasnow et al., 2013). The *Tac2* riboprobe was labeled with fluorescein and the *PKCd* and *Enk* with digoxigenin. Following a prehybridization procedure, the sections were hybridized with both riboprobes at 65°C for 16 h and then subjected to a series of stringent washes. Sections were then incubated with anti-fluoresceinpolymerized horse-radish peroxidase (POD) and Fab fragments, followed by fluorescent amplification and peroxidase quenching, and then with anti-digoxigenin-POD, Fab fragments (Roche). Signals were amplified with the TSA Plus Fluorescein Fluorescence System or TSA Plus Cy5 Fluorescence System (PerkinElmer) following each series of primary antibodies. Sections were then stained with DAPI (1:1000), washed, and coverslipped with Mowiol mounting medium. Immunofluoresence images were visualized and captured using Nikon eclipse TE300 microscope with a high resolution digital camera (Nikon, Melville, NY, USA). Confocal laser scanning microscopy was used to obtain high-resolution photomicrographs using an Orca R2 cooled CCD camera (Hammamatsu,Bridgewater, NJ, USA) mounted on a Leica DM5500B microscope (Leica Mircosystems, Bannockburn, IL, USA).

Amygdala cell culture

Amygdala primary cell culture from mice was performed as previously described (Mou et al., 2011).

All procedures involving animals were conducted in accordance with the NIH Guide for the Care and Use of Laboratory Animals. C57BL/6J mice (21 days postnatal) were decapitated, and amygdala was removed and immersed in ice-cold dissection buffer consisting of Hibernate-A medium (BrainBits, Springfield, IL, USA), B27 supplement (Invitrogen, Carlsbad, CA, USA), 2 mM Glutamax (invitrogen), and gentamycin (invitrogen) (12 μg/ mL) for the preparation amygdala neuronal cell cultures. The amygdala tissue was sliced and then enzymatically digested with papain (Worthington, Lakewood, NJ, USA) in Hibernate-A medium at 32°C for 30 minutes. Cells were dissociated by triturating with pasteur pipettes fired on tips to narrow openings. Neurons were purified in a density gradient media including Hibernate-A and OptiPrep (Sigma, St. Louis, MO, USA) by centrifugation. The density gradient media consisted of four layers. The first was 1 ml dissection buffer containing 35% OptiPrep; the second 1 ml dissection buffer contained 25% OptiPrep; the third 1 ml dissection buffer contained 20% OptiPrep; and the fourth 1 ml dissection buffer contained 15% OptiPrep. They were added on the top of each other carefully, resulting in clear layer separation. Then, cells were added on the top of density gradient media. After centrifugation, the most dense layer with a cream color, located at the middle of tube, could be seen. This layer of neurons was taken out by using a sterile transfer pipette and put into a new tube. After washing with dissection buffer, neuronal cells were plated onto Poly-D-Lysine (Sigma) coated plates or glass coverslips at the density of 2.5 × 105 cells / cm2 in culture media consisting of Neurobasal A medium (Invitrogen) with 2% B27 supplement, 2 mM glutamax and gentamycin (5 μg/mL). Thereafter, the cultures were kept in a humidified incubator at 37°C and 5% CO2, and media were changed every 5 days until used for experiments. After 2–3 weeks in vitro, the cells were used for the experiments reported in the present study.

Viability of neuronal cultures

Neurons were kept in the incubator for 2 weeks post-dissection, at which point 4% Trypan blue solution (Mediatech Inc., Herndon, VA, USA) was added onto cells to test the cell viability. Trypan blue positive dead cells were counted relative to the total number of cells. There were very few (<1%) dead cells, suggesting a >99% viability of cells at the 2-week timepoint. To determine ratio of neurons to total plated

cells at the time of isolation, cells were incubated for 12 hours to let them attach the well, then fixed with methanol at −20°C for 20 minutes. For the 2-week timepoint, cells were grown in vitro for two weeks, then fixed and stained in a similar manner. Following fixation, cells were stained with neuronal specific, mouse anti-NeuN and subsequently with goat anti-mouse Alexa Fluor 488. At the time of isolation (12 hrs post isolation) we found that ~90% of the DAPI+ cells were NeuN positive. After 2 weeks in culture, we found that ~73% of the DAPI+ cells were NeuN positive. Thus, we can assume that approximately ~75% of the cells the study outlined within this manuscript were neuronal (Mou et al., 2011).

Immunocytochemistry

Immunocytochemistry was performed as previously described (Mou et al., 2011). The antibody used was Pep2/ProNkB IHC (IS-39 ab, 1:500) (Kallo et al., 2012) and DAPI or NeuN (1:1000). This protocol began with changing half the culture media with fresh media and incubating cultures with polyclonal rabbit antisera against NkB. Cells were incubated for 30 minutes at 37°C. After washing three times with dissection buffer, culture media was returned to cells with half fresh media. To label NkB cells were incubated with goat anti-rabbit IgG conjugated with Alexa Fluor 488 (Invitrogen, 1:2000) diluted in culture media for 20 minutes in incubator. Cells were then rinsed three times with ice-cold PBS on ice and fixed with methanol at −20°C for 20 minutes. Following washing with PBS, cells were incubated with blocking buffer (1% BSA and 3% normal goat serum in PBS) at room temperature for 1 hour. All subsequent antibodies were diluted in the blocking buffer. To detect NkB the goat anti-rabbit IgG conjugated with Alexa Fluor 568 (Invitrogen, 1:2000) was applied to cells for additional 1 hour at room temperature. Cells without primary antibody treatment and only the above secondary were used as negative controls. Immunofluoresence images were visualized and captured using Nikon eclipse TE300 microscope with a high resolution digital camera (Nikon, Melville, NY, USA). The relative immnofluorescence intensity was analyzed using software of NIS-Elements BR2.30 (Nikon).

Immunohistochemistry

Pep2/ProNkB (IS-39 ab, 1:500) was the antibody used to detect NkB. The procedure was adapted from the one followed as previously described (Kallo et al., 2012). The procedure for detecting Gad65 (AB5082, Chemicon, 1:500) and CaMKII (Cell Signalling Solutions, 1:250) was followed similarly as previously described (Jasnow et al., 2013) and performed after the FISH(Jasnow et al., 2013). Brain sections (16 μm) on slides (described above) were incubated with PBS and Triton X-100, blocked with normal goat serum, bovine serum albumin, and Triton X-100, and incubated in a 1:500 dilution of primary antibody overnight at 4°C. Sections were then washed with PBS and bathed in a 1:500 dilution of secondary anti-rabbit biotinylated antibody (Ab) for 2 hr or Alexa Fluor® 568 Goat Anti-Rabbit IgG (Invitrogen 1:500). Avidin–biotin complexes were amplified using a standard Vectastain Elite ABC kit and visualized with diaminobenzidine (DAB) peroxidase staining. Sections were washed, and coverslipped with Mowiol mounting medium. images were visualized and captured using Nikon eclipse TE300 microscope with a high resolution digital camera (Nikon, Melville, NY, USA). Confocal laser scanning microscopy was used to obtain high-resolution photomicrographs using an Orca R2 cooled CCD camera (Hammamatsu,Bridgewater, NJ, USA) mounted on a Leica DM5500B microscope (Leica Mircosystems, Bannockburn, IL, USA).

ELISA

Purchased from Mybiosource, Mouse Neurokinin B ELISA Kit (NKB), Catalogue #MBS744693. Inter-assay CV%: 7.5-8.6, Intra-assay CV%: 8.2-9.5, Spike Recovery: 95-103%. Procedure was followed as indicated by the manufacturer.

Production of Recombinant Viral Vectors

Viral vectors are derived from the human immunodeficiency virus-based lentiviral backbones. The lenti-GFP viral plasmid was the “FUGW” vector (Huang et al., 2013). FUW-*Tac2* was created by replacing

GFP by the *Tac2* coding sequence, 0.72 kb EcoRI–XhoI fragment, in the FUGW vector (Rattiner et al., 2004). HEK 293FT (Invitrogen) cells were maintained in complete medium (4.5g/L Glucose and L-Glutamine containing DMEM supplemented with 10% FBS and 1% Pen-Strep) and incubated at 37ºC, 5% CO2. One day before transfection, HEK 293FT cells were seeded onto ten 150mm plates at a density of 1x107 cells per plate in 20 ml of complete medium. The cells were approximately 70-80% confluent at the time of transfection. The day of transfection, mixture prepared as the following: 250ug of FUGW or FUW-*Tac2* + 187.5ug of pCMVdelta 8.9 + 75ug of pV-SVG + 12ml of ddH2O + 12.5ml of 0.5M Ca2Cl + 25 ml of 2x HeBS to total volume 50ml, this solution was vortexed a few seconds and incubated for 20min at room temperature, and then 5ml of the mixture added dropwise to the each dish, dishes were returned to incubator. 7 hours post-transfection, the medium was replaced with 20 ml of fresh medium and incubated for an additional 48 h before harvesting. The supernatant containing lentivirus were collected 2 days after 48h and 72h post-transfection, 2 days supernatant were combined and was centrifuged at 500xg for 5min at 40ºC, followed by passage through a 0.45um low protein binding filter. The total 400ml of supernatant was loaded to six 70ml ultracentrifuge tubes in centrifuged at 28,000rpm for 2h at 40C in a 45Ti rotor (Beckman). The virus pellets were resuspended in 500ul of PBS, incubated on ice for 30min, six tubes of resuspended virus were combined, and then loaded it to a 12ml of SW 41 tube, 3ml of 20% sucrose added as a cushion, then centrifuged at 28,000rpm for 2h at 40C in a SW 41 rotor (Beckman). The virus pellet was resuspended in 100ul of PBS, incubated for 2h at 40C, then aliquot it and saved at -80ºC. Procedure was followed as previously described (Huang et al., 2013). The pAAV-hSyn-double floxed hM4D-mCherry (hM4Di-mCherry AAV) was purchased from UNC Gene Therapy Center, NC, USA).

Stereotaxic surgery and injection of virus

Mice were anesthetized by i.p. injections of a Ketamine – Domitor (medetomidine) mixture and placed in a stereotaxic apparatus. CeA coordinates were as follows: anteroposterior, -1.34mm; dorsoventral, -4.4mm; mediolateral, - 2.4mm relative to bregma. For the Lv-*Tac2* experiments the animals received bilateral intra-CeA amygdala injections of lentiviral vectors expressing *Tac2*-FUW or FUGW (GFP) in 1%

BSA in phosphate buffered saline (PBS) 0.5 µl of virus/side. 1 µl of virus/side of the pAAV-hSyn-double floxed hM4D-mCherry (hM4Di-mCherry AAV) was injected in the CeA of *Tac2*-Cre- and *Tac2*-Cre+ mice. For all experiments the rate of injection was 0.1 µl/min and the needle was left in place for 10 min following injection and the skin was closed using a 6-0 Vicryl suture.

Drugs administration

The Nk3R antagonist osanetant (Axon Medchem) was dissolved in physiological saline and 0.1% Tween 20 which was also the vehicle. Intraperitoneally (i.p.) dose was 5 mg/kg for systemic administration. Clozapine-N-oxide (CNO, Sigma Aldrich C0832) was given i.p. at 1mg/kg (Krashes et al., 2011).

Stereotaxic surgery and intra-cerebral cannulation

Mice were anesthetized by i.p. injections of a Ketamine – Domitor (medetomidine) mixture and placed in a stereotaxic apparatus. Small holes were drilled into the skull and 6 mm stainless-steel guide cannulas (Plastics One) were lowered bilaterally in to the Central Amygdala (CeA). CeA coordinates were as follows: anteroposterior, -1.34mm; dorsoventral, -4.4mm; mediolateral, - 2.4mm relative to bregma (Andero et al., 2013). Dorsoventral coordinates were measured from the skull surface with the internal cannula extending 2 mm beyond the end of the guide cannula. The guide cannula was fixed to the skull using dental acrylic and jeweler's screws and dummy cannulas (Plastics One) were inserted into each guide cannula to prevent clogging. All animals were allowed to recover for 14 days before testing. During this time, mice were handled daily for acclimation and inspection of cannula fixture. Intracerebral Infusions of 0.5 µl of drug or vehicle were made using an injection cannula (33 gauge cannula, Plastics One), which extended 2.0 mm beyond the tip of the guide cannula. Osanetant was delivered manually with a 5 µl Hamilton syringe attached to the injection cannula via polyethylene tubing (PE-10). Administration of a volume of 0,5 µl/side was delivered over a period of 60 seconds by slowly turning the microsyringe plunger. 625 ng of osanetant per side was injected. After each infusion, the injection cannula was allowed to remain

for 2 minutes. After finishing the behavioral studies mice where perfused with 4% paraformaldehyde. After fixation, brains were equilibrated in 30% sucrose, sectioned on a cryostat and stained with cresyl violet. Visualization of the cannula placement was performed on a light microscope to verify its location. Dots indicate the lowest point of the injector tip for each mouse for each group.

Statistics

Statistics were performed with IBM SPSS Statistics 19.0. Detection of outliers was performed and, when necessary, removed from analyses. ANOVA followed by post-hoc analyses were appropriate, repeated-measures ANOVA or Student's t test (two-tailed) for independent samples was tested. The results are presented as means ± or + SEM, and statistical significance was set at $P \leq 0.05$.